

Structure-based Design and Synthesis of Novel Furan-Diketopiperazine-Type Derivatives as Potent Microtubule Inhibitors for Treating Cancer

Zhongpeng Ding, Feifei Li, Changjiang Zhong, Feng Li, Yuqian Liu, Shixiao Wang, Jianchun Zhao, Wenbao Li

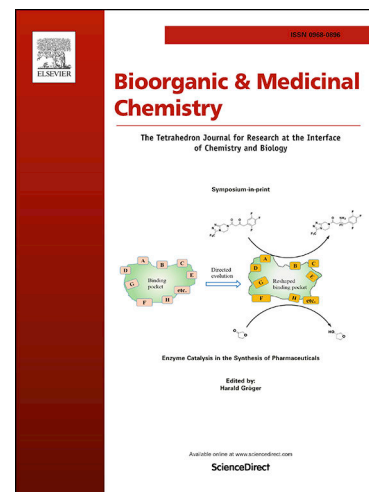
PII: S0968-0896(20)30245-5
DOI: <https://doi.org/10.1016/j.bmc.2020.115435>
Reference: BMC 115435

To appear in: *Bioorganic & Medicinal Chemistry*

Received Date: 4 January 2020
Revised Date: 10 March 2020
Accepted Date: 10 March 2020

Please cite this article as: Z. Ding, F. Li, C. Zhong, F. Li, Y. Liu, S. Wang, J. Zhao, W. Li, Structure-based Design and Synthesis of Novel Furan-Diketopiperazine-Type Derivatives as Potent Microtubule Inhibitors for Treating Cancer, *Bioorganic & Medicinal Chemistry* (2020), doi: <https://doi.org/10.1016/j.bmc.2020.115435>

This is a PDF file of an article that has undergone enhancements after acceptance, such as the addition of a cover page and metadata, and formatting for readability, but it is not yet the definitive version of record. This version will undergo additional copyediting, typesetting and review before it is published in its final form, but we are providing this version to give early visibility of the article. Please note that, during the production process, errors may be discovered which could affect the content, and all legal disclaimers that apply to the journal pertain.



Graphical Abstract

To create your abstract, type over the instructions in the template box below.

Structure-based Design and Synthesis of Novel Furan-Diketopiperazine-Type Derivatives as Potent Microtubule Inhibitors for Treating Cancer

Zhongpeng Ding ^a, Feifei Li ^a, Changjiang Zhong ^a, Feng Li ^c, Yuqian Liu ^a, Shixiao Wang ^d, Jianchun Zhao ^{a, d} and Wenbao Li ^{a, b, d*}

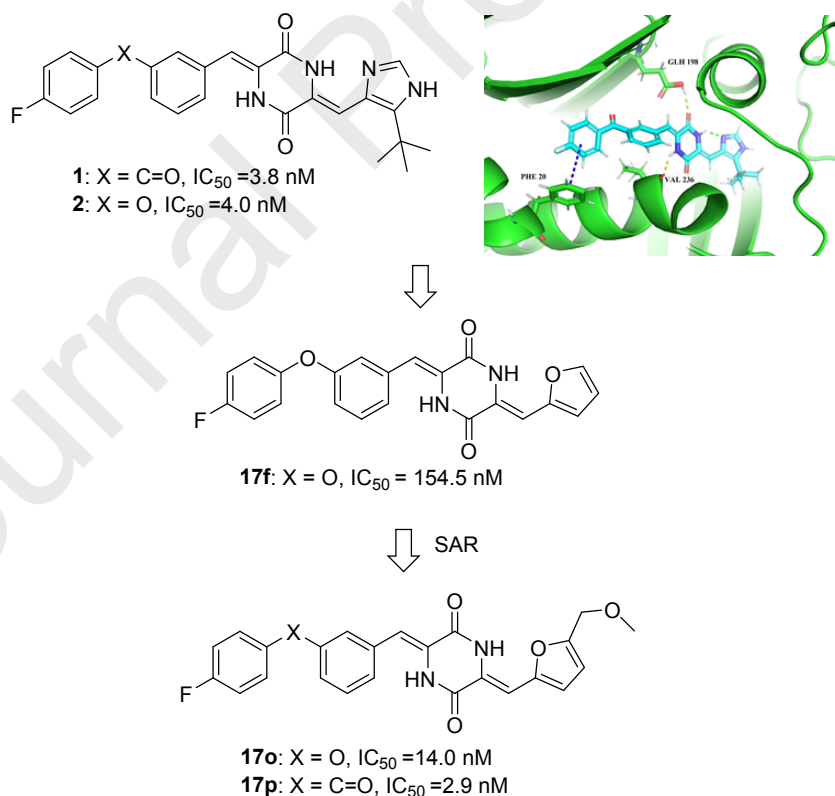
^a School of Medicine and Pharmacy, Ocean University of China, Qingdao 266003, China

^b Innovation Center for Marine Drug Screening and Evaluation, Qingdao National Laboratory for Marine Science and Technology, Qingdao 266071, China

^c Shandong Peninsula Engineering Research Center of Comprehensive Brine Utilization, Weifang University of Science and Technology, Weifang 262700, Shandong, China.

^d Marine Biomedical Research Institute of Qingdao, Qingdao 266071, China

* Corresponding author: *Tel:* 86-532-85906861; *E-mail:* wbli92128@ouc.edu.cn (Wenbao Li)



Leave this area blank for abstract info.

Fonts or abstract dimensions should not be changed or altered.



Structure-based Design and Synthesis of Novel Furan-Diketopiperazine-Type Derivatives as Potent Microtubule Inhibitors for Treating Cancer

Zhongpeng Ding ^a, Feifei Li ^a, Changjiang Zhong ^a, Feng Li ^c, Yuqian Liu ^a, Shixiao Wang ^d, Jianchun Zhao ^{a, d} and Wenbao Li ^{a, b, d*}

^a School of Medicine and Pharmacy, Ocean University of China, Qingdao 266003, China

^b Innovation Center for Marine Drug Screening and Evaluation, Qingdao National Laboratory for Marine Science and Technology, Qingdao 266071, China

^c Shandong Peninsula Engineering Research Center of Comprehensive Brine Utilization, Weifang University of Science and Technology, Weifang 262700, Shandong, China.

^d Marine Biomedical Research Institute of Qingdao, Qingdao 266071, China

* Corresponding authors: Tel: 86-532-85906861; E-mail: wbli92128@ouc.edu.cn (Wenbao Li)

ARTICLE INFO

Article history:

Received

Received in revised form

Accepted

Available online

Keywords:

Structure-based Drug Design

Furan-Diketopiperazine-Type

SAR

Microtubule Inhibitor

Anticancer

ABSTRACT

Plinabulin, a synthetic analog of the marine natural product “diketopiperazine phenylahistin,” displayed depolymerization effects on microtubules and targeted the colchicine site, which has been moved into phase III clinical trials for the treatment of non-small cell lung cancer (NSCLC) and the prevention of chemotherapy-induced neutropenia (CIN). To develop more potent anti-microtubule and cytotoxic derivatives, the co-crystal complexes of plinabulin derivatives were summarized and analyzed. We performed further modifications of the *tert*-butyl moiety or C-ring of imidazole-type derivatives to build a library of molecules through the introduction of different groups for novel skeletons. Our structure-activity relationship study indicated that compounds **17o** (IC₅₀ = 14.0 nM, NCI-H460) and **17p** (IC₅₀ = 2.9 nM, NCI-H460) with furan groups exhibited potent cytotoxic activities at the nanomolar level against various human cancer cell lines. In particular, the 5-methyl or methoxymethyl substituent of furan group could replace the alkyl group of imidazole at the 5-position to maintain cytotoxic activity, contradicting previous reports that the *tert*-butyl moiety at the 5-position of imidazole was essential for the activity of such compounds. Immunofluorescence assay indicated that compounds **17o** and **17p** could efficiently inhibit microtubule polymerization. Overall, the novel furan-diketopiperazine-type derivatives could be considered as a potential scaffold for the development of anti-cancer drugs.

2009 Elsevier Ltd. All rights reserved.

1. Introduction

Cancer has become the primary cause of human death in the world. There were 17.0 million reported cancer cases and 9.5 million cancer-related deaths globally in 2018, and it is estimated that the number of new cancer cases will reach 27.5 million by 2040¹. There were 3.93 million cancer cases and 2.34 million cancer-related deaths reported in China in 2015. Microtubule targeting agents were discovered through in-depth

and systematic research and currently are divided into four categories based on their binding sites (i.e. taxanes, vinblastines, colchicines and laulimalids)²⁻⁴. Microtubule inhibitors exhibited highly potent anti-microtubule and cytotoxic activities by stabilizing or disaggregating microtubule polymerization in the process of microtubule assembly, a property which could disrupt the dynamic balance

cell division⁵⁻⁷. Vinca alkaloid site-binding agents and taxane site-binding agents have been widely used to treat various cancers^{8,9}. However, severe neurotoxicity, adverse myelosuppression effects, and multidrug resistance have also been observed in their clinical applications⁸⁻⁹. In contrast, molecules binding at colchicine sites have not yet been developed into clinical cancer therapies.

Plinabulin, a micro-tubulin inhibitor derived from the marine natural product “phenylahistin,” has been moved into phase III clinical trials paired with docetaxel as a combination agent for treating non-small cell lung cancer (NSCLC) and for the prevention of chemotherapy-induced neutropenia (CIN). The treatment could block cells in the G2/M phase of the cell cycle and induce apoptosis through caspase-3, caspase-8, caspase-9, and PARP (poly ADP-ribose polymerase) cleavage¹⁰⁻¹³. Importantly, plinabulin was also shown to inhibit tumor cell proliferation through the disruption of tumor vascular endothelial cells¹⁴. Recent studies reported that plinabulin binds at the colchicine site of tubulin to prevent the assembly of α/β -tubulin heterodimers and induces GEF-H1 release to increase dendritic cells from driving a distinct cell signaling program^{15,16}.

The co-crystal complex of plinabulin with tubulin (PDB code: 5C8Y) was cultured and resolved at different resolutions by Yang et. al and Cavalli et. al, which could elucidate the detailed interactions between ligands and tubulin^{16,17}. The crystal structures of the tubulin complex with plinabulin derivatives (KPU-105, MBRI-001, compound **1**) were also solved and reported previously, for which PDB codes were 5YL4, 5XI5, and 5XHC, respectively. These tubulin–ligand complex structures revealed that plinabulin derivatives resided in a deeper position in β -tubulin, which primarily contributed to the binding affinity of ligands and tubulin. The carbonyl oxygen atom and the hydrogen atom on the nitrogen of diketopiperazine (DKP) of plinabulin derivatives could form

respectively¹⁸⁻²¹. In crystal structures (5YL4 and 5XHC), the benzene ring of the benzoyl group on the A ring could form an additional π - π interaction, which could be beneficial to anti-proliferation^{18,20}. The pocket at the colchicine site crossed the α/β -tubule subunit and extended to the boundary of the GTP pocket, which was formed from the hydrophilic and hydrophobic amino acid residues¹⁹⁻²¹. Among these amino acid residues around the binding pocket of plinabulin derivatives, the conformation of the T7 loop (amino acid residue number: 244-251) and H7 helix (amino acid residue number: 224-243) in β -tubulin was changed in comparison with the structure of tubulin-apo, which may primarily contribute to the inhibition of microtubule polymerization¹⁹. Therefore, the position of 5-*tert*-butyl-*1H*-imidazole of the C-ring, which was close to the tubulin heterodimer interface, had an important influence on tubulin conformation.

A systematic structure-activity relationship study (SAR) of plinabulin derivatives were performed by Hayashi's group, in which compound **1** ($IC_{50} = 3.8$ nM, NCI-H460) was reported to have the most potent anti-proliferation activity^{13,22-23}. Our group also designed and synthesized three series of A/B/C-ring plinabulin derivatives based on the co-crystal structures. So far, compound **2** ($IC_{50} = 4.0$ nM, NCI-H460) was the optimally active compound, and the theoretically calculated LogPo/w and PCaco were superior to other compounds²⁰. In general, plinabulin derivatives exhibited optimal activities when the C-rings had 5-*tert*-butyl *1H*-imidazole and 2-pyridine (KPU-300, $IC_{50}=7.0$ nM, HT-29, $IC_{50}= 6.3$ nM, BxPC-3). In particular, the *tert*-butyl group at the 5-position of imidazole was essential for the activity of such compounds. To further understand the SAR of plinabulin derivatives and to obtain more potent compounds, we further analyzed the co-crystal structure of compound **1** with tubulin, then designed and modified the C ring in this study.

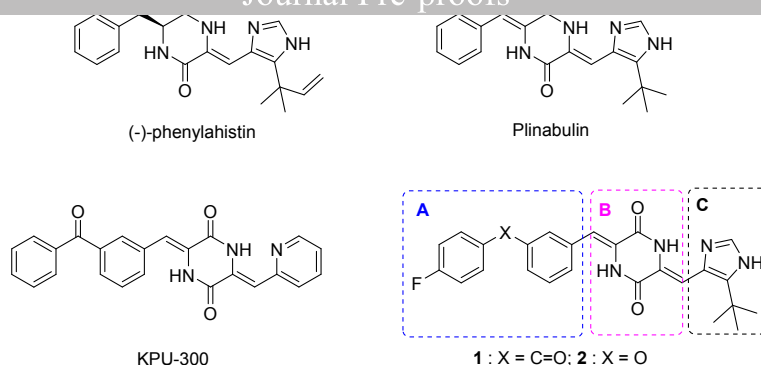


Fig. 1. Chemical structures of (-)-phenylahistin, plinabulin and its representative derivatives.

2. Results and discussion

2.1. Analysis of Co-crystal complex of compound **1** with tubulin and design strategy

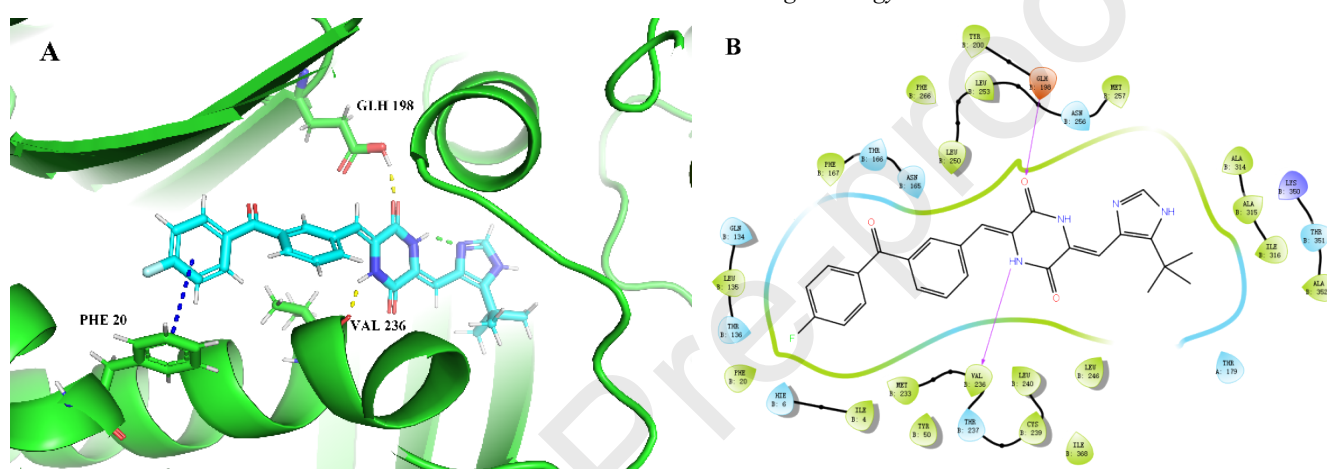


Fig. 2. Co-crystal structure of tubulin with compound **1** in different visual display.

The co-crystal complex of compound **1** at 2.75 Å resolution was reported and placed in a protein data bank (PDB, <https://www.rcsb.org/structure/5XHC>), which brought new insight to the interaction of microtubules and the molecule²⁰. In this study, the co-crystal complex was further analyzed by computer calculation using Maestro software (Fig. 2). Compound **1** could form favorable interactions with tubulin, including hydrogen bonding and π - π interactions. The majority hydrophobic residues included ALA314, ALA315, ILE316, LEU246, LEU240, VAL236, MET233, ILE4, PHE20, LEU135, PHE167, LEU250, and MET257, and the majority hydrophilic residues included THR179, HTE6, THR136, GLN134, THR166, ASN165, and ASN256 from α tubulin or β tubulin, both of which could form a protein pocket. Moreover, the pocket that crossed the α/β -tubule subunit and extended to the boundary of the GTP

pocket could provide more space for further modification of 2, 5-diketopiperazine derivatives.

According to the previous report, the pharmacophore of the A ring was optional to the *para*-fluorobenzoylphenyl or *para*-fluorophenoxyphenyl group, and the diketopiperazine core structure of the B ring was immutable if their favorable interactions were to be maintained^{20, 22}. In this study, we expanded upon these findings and designed four series of compounds with different C ring substitutions with which to explore the new scaffolds and structure-activity relationship (SAR). The 5-position of imidazole was replaced by different alkyl groups in series 1 to confirm the function of the *tert*-butyl group, and series 2-4 were constructed to explore different types of aromatic rings at the C ring.

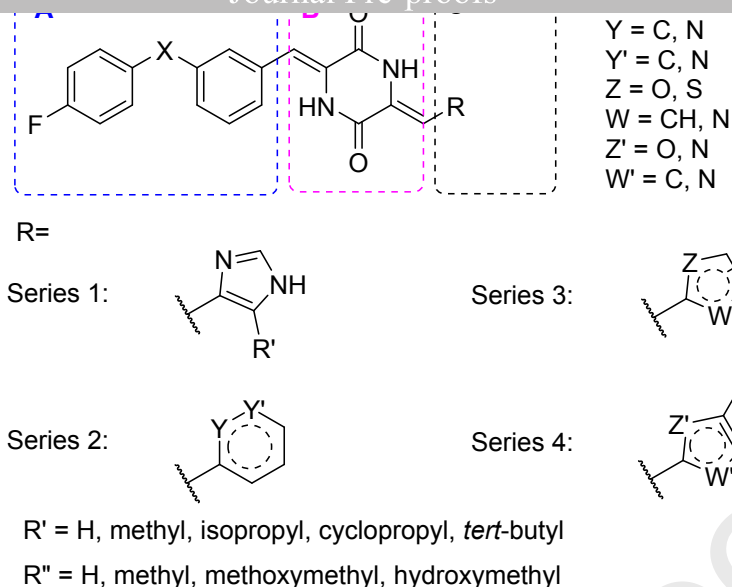


Fig. 3. General design structures of compounds **14a-14h** and compounds **17a-17r**.

2.2. Chemistry

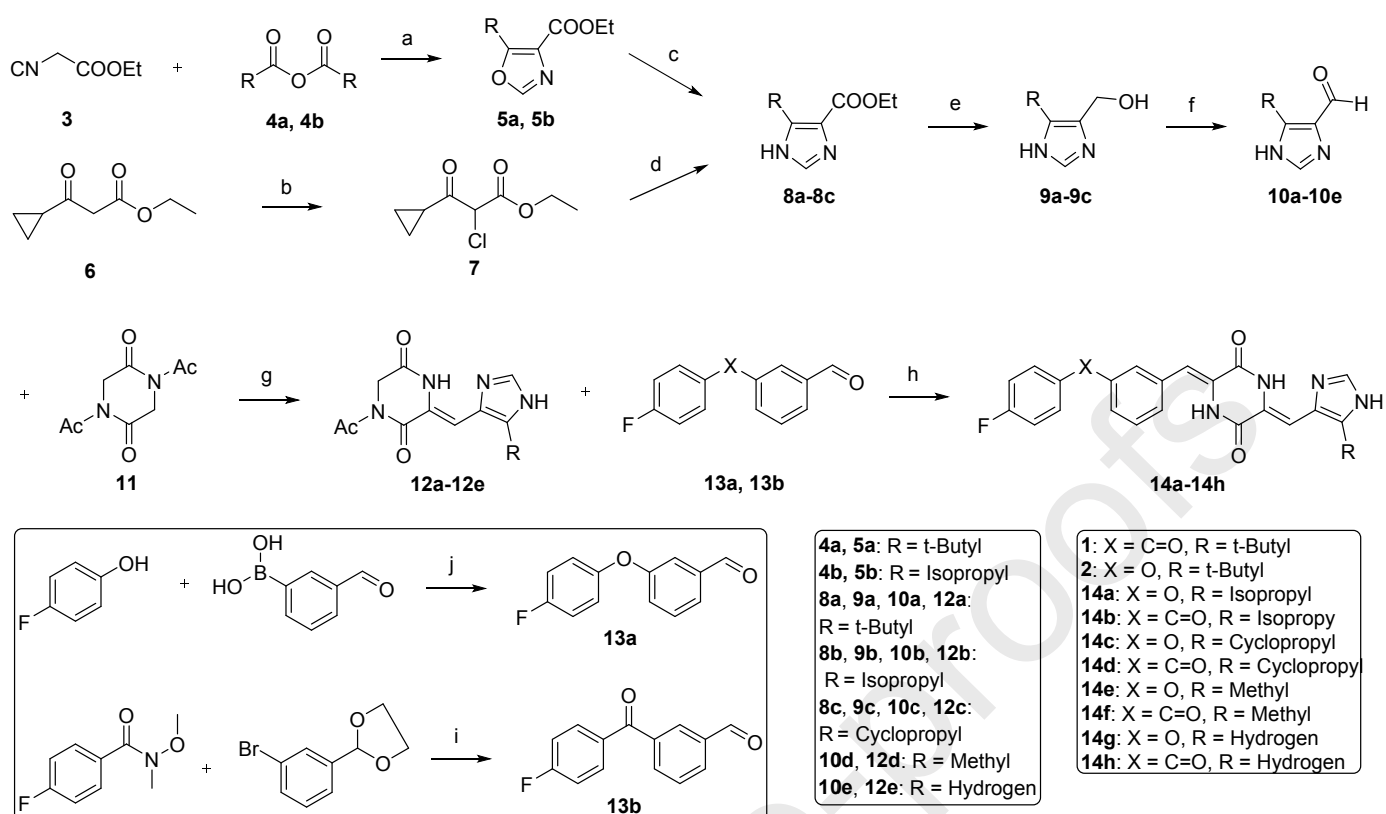
To synthesize the plinabulin derivatives **1**, **2**, **14a-14h**, and **17a-17r**, we explored and adopted two synthetic strategies to condense the A ring and C ring with DKP. The two routes could be used for different aldehydes, dependent upon improved yield and fewer by-products of the reaction. The chemical structures of the compounds were characterized by nuclear magnetic resonance (NMR) and high-resolution mass spectrometer (HRMS) analysis (see Supporting Information).

2.2.1. Synthesis of plinabulin derivatives **1**, **2** and **14a-14h**

The plinabulin derivatives **1**, **2**, and **14a-14h** were synthesized via a sequence of six linear steps. Firstly, the colorless liquid oxazole esters **5a** and **5b** were synthesized through a [3 + 2] cyclization reaction using ethyl 2-cyanoacetoacetate and pivalic anhydride or isobutyric anhydride as the starting materials in the presence of 1, 8-diazabicyclo[5.4.0]undec-7-ene (DBU) for 48 h at room temperature (approximately 20°C), and then purified by silica gel column chromatography. The oxazole ester was converted into the imidazole ester by the solvolysis reaction in formamide for 24 h at 175 °C, which was purified by slurry using water. Then, the imidazole ester was reduced to alcohol using LiAlH₄ as the reducing agent, and the aldehyde was generated by an oxidation

reaction using MnO₂. The intermediate **8c** was prepared through substitution and cyclization reactions in two consecutive steps. The pure **8c** was precipitated from water by adjusting the pH using aqueous sodium carbonate solution.

Consecutive aldol reactions with two different aldehydes onto the diacetyl-2, 5-piperazinedione ring were then carried out in the presence of Cs₂CO₃ in N, N-dimethylformamide (DMF). Namely, the various imidazole aldehydes were condensed with diacetyl-2, 5-piperazinedione for 20 h at room temperature. When the alkyl group was *tert*-butyl, cyclopropyl or isopropyl, the diacetyl-2, 5-piperazinedione was reacted with a single imidazole aldehyde. However, the reaction can produce double imidazole-3, 6-yl piperazine-2, 5-dione as a by-product when hydrogen or methyl occupies the 5- position of imidazole because of the resulting small steric hindrance. The by-product of the unsubstituted imidazole was greater than that of methyl imidazole and was difficult to purify through silica gel column chromatography. Therefore, the results indicated that the bulky group at the 5-position was important for preventing the formation of by-products. The final condensation reaction was performed in dark conditions under an N₂ atmosphere to avoid yielding a product of E configuration¹³. In general, the total yields of the synthesis of compounds **14a-14h** were above 1% in six steps.



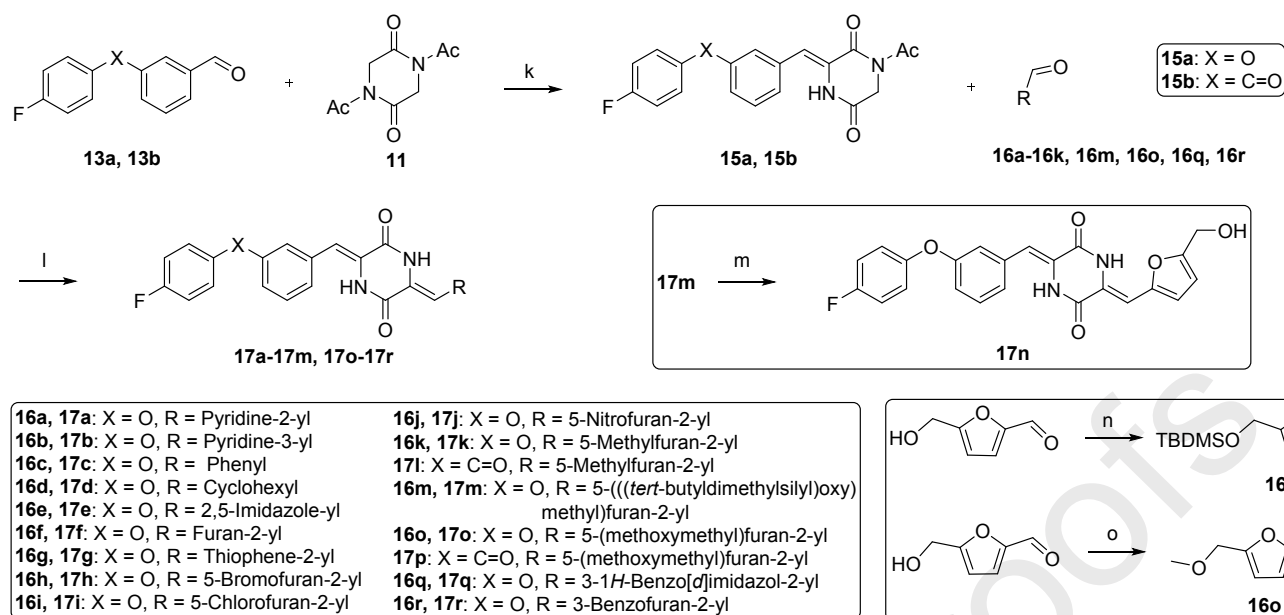
Scheme 1. Synthesis of plinabulin derivatives **1, 2, 14a-14h** and intermediate aldehydes **13a-13b**. Regents and conditions: (a) DBU, THF, rt, 48 h, 95-99%; (b) SOCl₂, CHCl₃, 0-65°C (reflux), 3 h, 97%; (c) formamide, 175°C, 36 h, 50-55%; (d) formamide, H₂O, 145°C, 20 h, 4%; (e) LiAlH₄, THF, 0°C to rt, 6 h, 94%-99%; (f) MnO₂, DCM, rt, 48 h, 43-72%; (g) Cs₂CO₃, Na₂SO₄, DMF, rt, 20 h, 39-50%; (h) Cs₂CO₃, Na₂SO₄, DMF, 45-50°C, 20 h, 23-70%; (i) 1) *n*-BuLi, THF, -78°C, 5 h; 2) HCl (1 M), THF, rt-40°C, 24 h; two steps yield 67%; (j) Cu(OAc)₂, Et₃N, DCM, rt, 48 h, 22%

2.2.2. Synthesis of plinabulin C-ring derivatives **17a-17r**

Route 2 details the synthesis of compounds **17a-17r**, which were produced according to the previous methods and strategies. The yield of by-products was high, and pure intermediates in quantity were difficult to obtain. We changed the synthesis strategy accordingly. Namely, the first aldehydes of ring A were reacted with DKP under nitrogen at room temperature for 20 h. In order to avoid the formation of isomers, the reactions were carried out in the absence of light to yield intermediates **15a** and **15b**. Both intermediates were used directly in the next reaction without further purification.

The second aldehydes were reacted with the intermediate **15a** or **15b** at 45-50 °C in the presence of Cs₂CO₃ in N, N-dimethylformamide (DMF). During the preparation of compound **17d**, less product was produced at 50 °C because of the lower reactivity of the cyclohexanecarboxaldehyde. The

reaction temperature was thus raised to 80°C to obtain the white solid compound **17d**. The reaction yield of compound **17j** (7 %) was very low in all reaction conditions because the strong electron-withdrawing action of its nitro group reduced the reactivity of furanaldehyde. Compound **17n** could not be obtained through a direct condensation reaction of 5-hydroxymethylfurfural with intermediate **15a**, which could be explained by the active hydroxyl group. To obtain the compound **17n**, the hydroxyl group of 5-hydroxymethylfurfural was protected with *tert*-butyldimethylsilyl and the 5-(*tert*-butyldimethylsilyloxymethyl) furfural (**16m**) was prepared in the presence of imidazole as a base at room temperature³; after reacting with **15a** to yield compound **17m**, the compound **17n** was obtained through the removal of the protective group by tetrabutylammonium fluoride (TBAF).



Scheme 2. Synthesis of plinabulin C-ring derivatives **17a-17r**. Regents and conditions: (k) Cs₂CO₃, Na₂SO₄, DMF, rt, 20 h, 47-77%; (l) Cs₂CO₃, Na₂SO₄, DMF, 45-80°C, 24 h, 7-75%; (m) TBAF (1 M), THF, rt, 5 h, 74%. (n) *tert*-butyldimethylsilyl chloride, imidazole, DCM, rt, overnight, 99%; (o) Methyl iodide, Cs₂CO₃, CH₃CN, 50°C, 24 h, 50%.

2.3. Cytotoxic activity

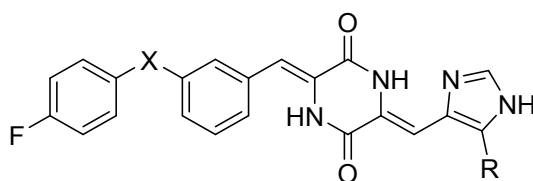
2.3.1. Biological activities of the synthesized plinabulin C-ring derivatives **1, 2** and **14a-14h**.

In order to explore the effect of *tert*-butyl moiety at the 5-position of imidazole, we synthesized a series of compounds in which the moiety was replaced by different alkyl groups. The activities of compounds **1, 2**, and **14a-14h** were evaluated by 3-(4, 5-dimethylthiazol-2-yl)-2, 5-diphenyltetrazolium bromide (MTT) assay against the human lung cancer NCI-H460 cell line (Table 1).

When the A ring was a *para*-fluorophenoxyphenyl group, compounds **2** (IC₅₀ = 4.0 nM), **14a** (IC₅₀ = 8.8 nM), or **14c** (IC₅₀ = 15.2 nM), which possessed *tert*-butyl, isopropyl, and cyclopropyl moiety at the 5-position of imidazole, respectively, displayed high cytotoxic activities. The IC₅₀ values of compounds **1, 14b**, and **14d** with the *para*-

fluorobenzoylphenyl group were 3.8 nM, 3.2 nM, and 2.8 nM, respectively. These results showed that the isopropyl and cyclopropyl moieties had the same activity as *tert*-butyl, and that the *para*-fluorobenzoylphenyl group and the *para*-fluorophenoxyphenyl group had similar contributions. However, when the *tert*-butyl was replaced by a methyl group, the activity of compound **14e** (IC₅₀ = 47.6 nM) was reduced 2-fold. A similar decrease was found in compound **14f** (IC₅₀ = 15.9 nM), the activity of which was less than that of compounds **1, 14b**, and **14d**. Further, when the 5-position of the imidazole was occupied by a hydrogen atom, the activities of the compounds **14g** (IC₅₀ = 478.5 nM) and **14h** (IC₅₀ = 277.5 nM) were decreased significantly. These results suggest that the large sterically hindered groups at the 5-position of imidazole were important for maintaining their activities, consistent with previously reported findings¹³.

Table 1. Biological activities of the synthesized plinabulin C-ring derivatives **1, 2** and **14a-14h**



Compounds	X	R	NCI-H460	QpLogPo/w	QpPCaco	score
Plinabulin			26.2 ± 3.2	2.5	377.8	11.7
2	O		4.0 ± 0.4	4.2	533.1	14.0
1	C=O		3.8 ± 1.2	3.6	265.7	15.0
14a	O		8.8±0.7	4.0	451.0	14.0
14b	C=O		3.2±0.9	3.3	137.9	14.6
14c	O		15.2±2.8	3.8	438.5	13.7
14d	C=O		2.8±1.1	3.1	214.1	14.8
14e	O		47.6±12.8	3.2	384.5	13.1
14f	C=O		15.9±4.8	2.6	191.1	13.8
14g	O	H	478.5±15.8	2.8	390.7	14.8
14h	C=O	H	277.5±2.0	2.1	168.2	13.3

^a Values represent mean ± SD from three independent dose response curves with NCI-H460 cancer cell line.

The absolute values of the docking scores of these derivatives ranged from 13 to 15, indicating that they might have similar activities. Table 1 displays the calculated PCaco of these diketopiperazine-type derivatives possessing *para*-fluorophenoxyphenyl groups, which were superior to the Pcac values of compounds with *para*-fluorobenzoylphenyl structures (i.e. 533.1 for compound **2** and 265.7 for compound **1**)²¹.

2.3.2. Biological activities of the synthesized plinabulin C-ring derivatives **17a-17r**.

To explore the effects of the new scaffold, the C-ring imidazole was replaced by a six-membered ring aromatic or

non-aromatic group, i.e. compound **17a**, **17b**, **17c**, or **17d**. The cytotoxic activity of compound **17a** (IC₅₀ = 49.1 nM) with 2-pyridine structure exhibited 10-fold less potency than compound **2** against the human lung cancer NCI-H460 cell line. Compounds **17b** and **17d** showed significantly decreased anti-proliferative activity, and the IC₅₀ values of these derivatives were higher than 1000 nM. In contrast, the IC₅₀ value of compound **17c** was 389.1 nM, which can be attributed to greater transmembrane activity in the cells due to this molecule's superior PCaco (1010.6). These results indicated that the six-membered ring substituents were not functionally equivalent to the *tert*-butyl-imidazole group.

series of five-membered aromatic ring groups were substituted for the imidazole C ring. The IC_{50} values of compounds **17e**, **17f**, and **17g** were >1000 nM, 154.5 nM, and >1000 nM, respectively. Compound **17e** (with 1H-5-imidazolyl group) exhibited significant inactivity and its theoretical calculated PCaco was inferior to the other two compounds. Although compound **17g** had a large transmembrane coefficient, it had almost no activity because the sulfur atom on thiophene cannot form a strong hydrogen bond with the NH of DKP. In contrast, compound **17f** (with furan group) could establish and maintain more potent cytotoxic activity with IC_{50} at 154.2 nM, in comparison with compound **14g**, with IC_{50} of 478.5 nM. These results indicate that the oxygen atom could form a hydrogen bond interaction with the NH of DKP in a planar pseudopentacyclic conformation, and the imidazole group could be replaced by a furan group to build a novel scaffold.

To further explore the structure-activity relationship, the electron-withdrawing substituents (such as bromo, chloro, and nitro) were synthesized to occupy the 5-position of furan, yielding compounds **17h-17j**. Compound **17h** (IC_{50} = 361.1 nM), with a bromine atom at the 5-position, exhibited an approximately 2-fold decrease in antiproliferative activity in comparison with compound **17f**. The IC_{50} value of compound **17i** (with chloro atom) was 180.3 nM, similar to that of compound **17f**. However, the cytotoxic activity of compound **17j** (with nitro group) was significantly decreased. This might be due to the strong electron-withdrawing group affecting the electron cloud distribution of the furyl oxygen atom, resulting in impeded hydrogen bond formation.

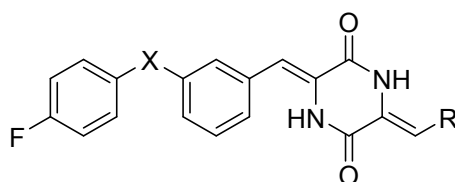
Compounds **17k-17p** were obtained with the substitution of an electron-donating group for the hydrogen atom at the 5-position of furan. The IC_{50} values of compounds **17k**, **17m**, **17n**, and **17o** were 30.0 nM, 377.7 nM, 41.5 nM, and 14.0 nM, respectively. Compound **17k** (with methyl group at 5-position

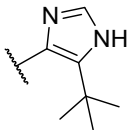
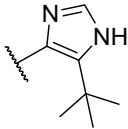
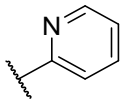
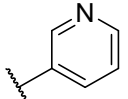
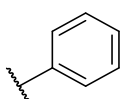
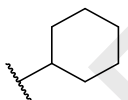
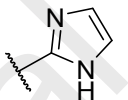
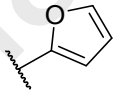
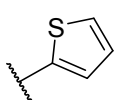
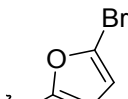
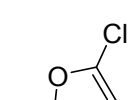
contrast, the anti-proliferative activity of compound **17m**, which had a large protective group, reduced about two-fold in potency. When the TBDMS protective group was removed from compound **17m**, the resulting compound (**17n**) possessed a hydrophilic hydroxyl structure and exhibited improved cytotoxic activity, equivalent to that of compound **17k**. The cytotoxic activity of compound **17o** (with methoxymethyl substituent group at the 5-position of furan) was increased ten-fold, displaying an activity (IC_{50} =14.0 nM) that was similar to previously reported compounds **2**, **14a**, and **14c**. These results indicate that the alkyl group of imidazole at the 5-position could be replaced by the methyl or methoxymethyl substituent of furan group, which is contradicting previous reports. The *para*-fluorophenoxyphenyl groups of Compounds **17k** and **17o** were substituted by *para*-fluorobenzoylphenyl structures to yield compounds **17l** and **17p**. Their IC_{50} values were 5.3 nM and 2.9 nM, respectively, which confirmed these activities. These results indicate that an appropriate electron-donating group occupying the 5-position of furan was important for maintaining the activity of novel furan-diketopiperazine-type derivatives.

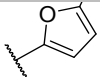
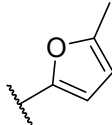
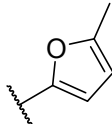
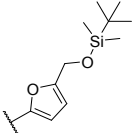
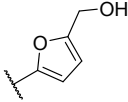
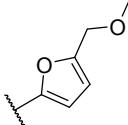
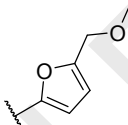
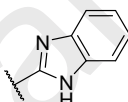
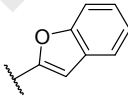
In light of the promising results described above, we designed and synthesized derivatives of imidazophenyl and furanophenyl (compounds **17q** and **17r**, respectively). In comparison with compound **17f**, compound **17r** decreased the potency significantly with an IC_{50} of 347.2 nM. Compound **17q** displayed a total loss of activity, with IC_{50} greater than 1000 nM.

In summary, compounds **17o** and **17p** had the best anti-proliferative activities in the novel scaffold derivatives. In addition, as reported in Table 1, the cytotoxic activities of compounds **2**, **1**, **14a**, **14b**, **14c**, and **14d** were also potent at the nanomolar level. We further explored their biological activities in different cancer cell lines.

Table 2. Biological activities of the synthesized plinabulin C-ring derivatives **17a-17r**



Compounds	X	R	NCI-H460	QLogPo/w	QPCaco	score
Plinabulin			26.2 ± 3.2	2.5	377.8	11.7
2	O		4.0 ± 0.4	4.2	533.1	14.0
1	C=O		3.8 ± 1.2	3.6	265.7	15.0
17a	O		49.1±4.7	3.9	799.8	13.3
17b	O		>1000 nM	3.6	649.5	13.0
17c	O		389.11±5.55	4.5	1010.6	13.1
17d	O		>1000 nM	4.6	515.3	12.7
17e	O		>1000 nM	3.0	383.1	12.7
17f	O		154.5±3.2	3.9	1012.9	12.7
17g	O		>1000 nM	4.4	1015.1	12.9
17h	O		361.1±8.3	4.5	1031.8	12.8
17i	O		180.3±5.2	4.4	1062.7	12.6

17j	O		>1000	3.2	118.3	13.0
17k	O		30.0±1.2	4.2	983.1	13.0
17l	C=O		5.3±0.3	3.5	486.4	13.7
17m	O		377.7±20.3	6.4	1619.8	10.4
17n	O		41.5±4.9	3.2	333.7	13.0
17o	O		14.0±0.2	4.0	1303.2	13.3
17p	C=O		2.9±1.1	3.4	274.1	13.9
17q	O		>1000 nM	3.9	441.3	13.1
17r	O		347.2±30.8	4.9	979.9	9.8

^a Values represent mean ± SD from three independent dose response curves with NCI-H460 cancer cell line.

2.3.3. Biological activities of plinabulin and different derivatives in various cancer cell lines

The cytotoxic activities of derivatives **1**, **2**, **14a-14d**, **14h**, **17l**, **17o**, and **17p** were further evaluated against various tumor cells, such as the pancreatic cancer BxPC-3 cell line and colon

cancer HT-29 cell line, by MTT assay. As shown in Table 3, compounds **1**, **2**, **14a-14d**, **14h**, **17l**, **17o**, and **17p** exhibited very potent activities against different cancer cell lines at nanomolar levels. For example, the IC₅₀ were 6.6 and 7.0 nM for compound **17o**, and 2.0 and 2.2 nM for compound **17p**.

Table 3. Biological activities of plinabulin and different derivatives **1**, **2**, **14a-14d**, **14h**, **17o** and **17p** in various cancer cell lines

Compds	IC ₅₀ ^a (nM) /BxPC-3	IC ₅₀ (nM)/ HT-29
Plinabulin	5.8±0.2	6.6±1.6

1	0.6±0.1	0.6±0.2
14a	3.4±0.3	3.7±0.3
14b	0.6±0.02	0.8±0.02
14c	9.4±1.5	7.4±0.01
14d	1.4±0.02	1.4±0.03
14h	4.3±0.2	5.1±0.6
17l	3.7±0.02	3.3±0.08
17o	6.6±1.1	7.0±0.9
17p	2.0±1.5	2.2±0.3

^a Values represent mean ± SD from three independent dose response curves with four human cancer cell lines.

2.4. Immunofluorescent assay

To further explore the effects of derivatives **1**, **2**, **14a**, **14b**, **17o**, and **17p** on microtubules in cancer cells, an immunofluorescence assay was performed. As shown in Figure 4, NCI-H460 cells were treated individually with Plinabulin (10 nM), compounds **2** (10 nM), **1** (2 nM), **14a** (10 nM), **14b** (10 nM), **17o** (10 nM), or **17p** (10 nM) for 24 h and then

stained for β -tubulin and DAPI. In comparison to the control, the microtubule networks had been damaged (Figure 4). The semi-quantitative calculations were performed through the software Image Pro Plus 6.0, and is shown in Figure 5. The inhibition activities were consistent with the anti-proliferative activities detailed previously.

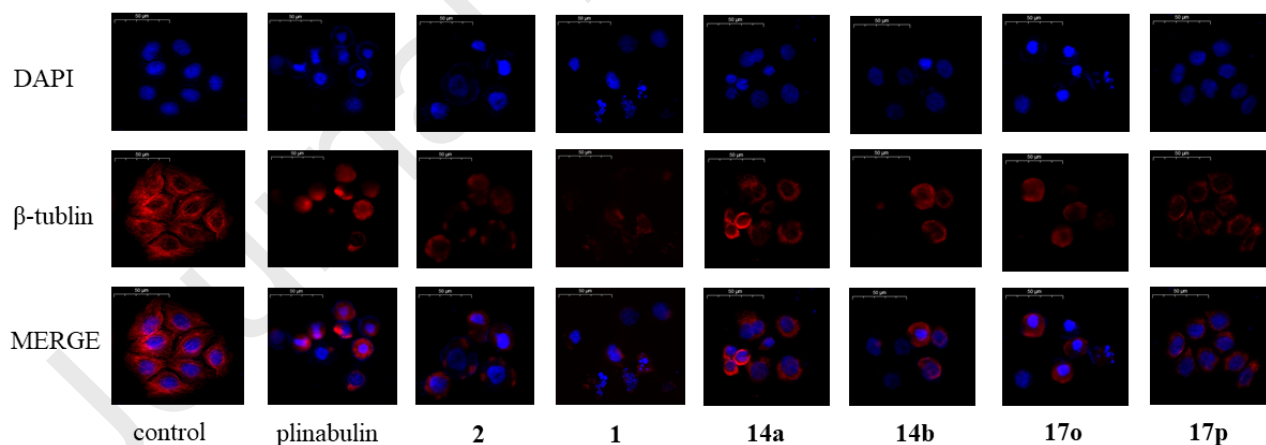


Fig. 4. Immunofluorescence assays of Plinabulin, compounds **1**, **2**, **14a**, **14b**, **17o** and **17p**. (a) NCI-H460 cells were treated with Plinabulin (10 nM), compounds **2** (10 nM), **1** (2 nM), **14a** (10 nM), **14b** (10 nM), **17o** (10 nM) and **17p** (10 nM) for 24 h and then stained for β -tubulin and DAPI. (i) Nuclear (blue); (ii) tubulin (red); (iii) (i) and (ii) were overlapped.

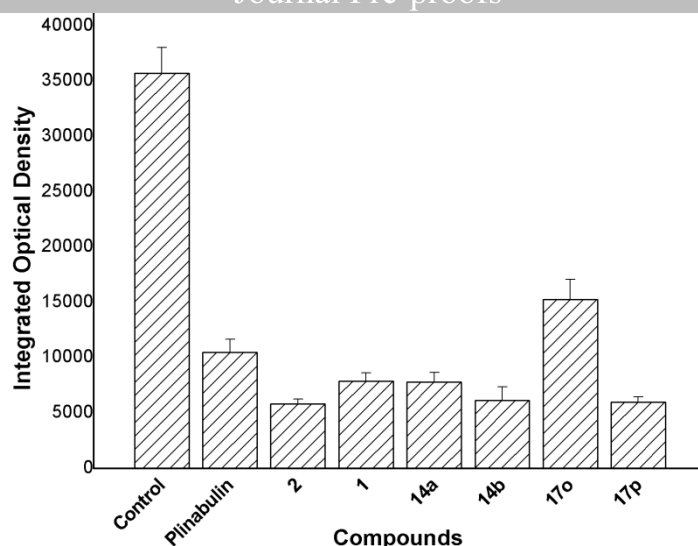


Fig. 5. Semi-quantitative analysis of the inhibition of tubulin polymerization plinabulin, compounds **1**, **2**, **14a**, **14b**, **17o** and **17p**.

2.5. Theoretical calculations and molecular docking

Theoretical calculations of the physical properties of these synthesized compounds were performed using the Qikprop Module of Maestro software. The interaction modes of compounds **1**, **2**, **14a-14h**, and **17a-17r** were investigated by molecular docking using Maestro software. The oil-water partition coefficient (LogPo/w), cell permeability (Pcaco), and docking score were calculated, and are shown in Table 1 and Table 2, respectively. The LogPo/w values of the derivatives were within the reasonable range of -2.0-6.5. The cell permeability of some compounds was greater than 100, which was beneficial for the improvement of activity.

The co-crystal structure of compound **1** is shown in Fig. 6B. The binding modes of compounds **14a** and **14c** with *para*-fluorophenoxyphenyl group were similar to that of compound **2**, which formed hydrogen bonds with amino acid residues (the carbonyl oxygen atom of VAL236 with the NH of DKP, and the hydrogen atom of the carboxylic acid of GLH198 with the oxygen atom of the carbonyl group of DKP in Fig. 6A). In contrast, compounds **1**, **14b**, and **14d** with *para*-fluorobenzoylphenyl structure were able not only to form the same hydrogen bond with amino acid residues, but also to form π - π interaction with the benzene ring of amino acid PHE20, as shown in Fig. 6B. In general, compounds **1**, **2**, and **14a-14h** had highly similar molecular conformations in the tubulin-binding pocket in Fig. 2A, 6C, 6D, 6E, 6F, 6G, respectively, which was able to form intramolecular hydrogen bonds. These results show that favorable interactions were

important to maintaining the activity of such compounds, and could support experiments investigating biological activities.

Figures 7A and 7B illustrate the similarity of compounds **2**, **17a**, and **17f** in terms of interaction and configuration. Table 2 shows in detail that compound **17f** (without a favorable alkyl group at 5-position of C ring) exhibited favorable biological activity in a series of compounds, which can be attributed to its better cell permeability (PCaco = 1012.86) in comparison with that of compound **2** (PCaco = 533.05). The volume of compound **17f** at the C ring was slightly smaller than compound **17a**, resulting in reduced cytotoxic activity. Compound **17g** had no cytotoxic activity because there was no strong intra-ligand hydrogen bond in the docking mode shown in Fig. 7C.

In addition, we found that the hydroxyl hydrogen atom of compound **17n** could form a hydrogen bond with the oxygen atom of ASN256, while the hydroxyl group occupied the interface of α/β -tubulin heterodimers, which could cause potent cytotoxic activity. This result indicates that the hydrophilic group could exist in the extension pocket of the interface. In contrast, the methoxymethyl substituent group at the 5-position of the furan of compound **17p** might have influenced the H8 and T7 loops to interfere with the microtubule assembly, which could perform the same function as the *tert*-butyl imidazole of compound **1**, shown in Fig. 8B¹⁹.

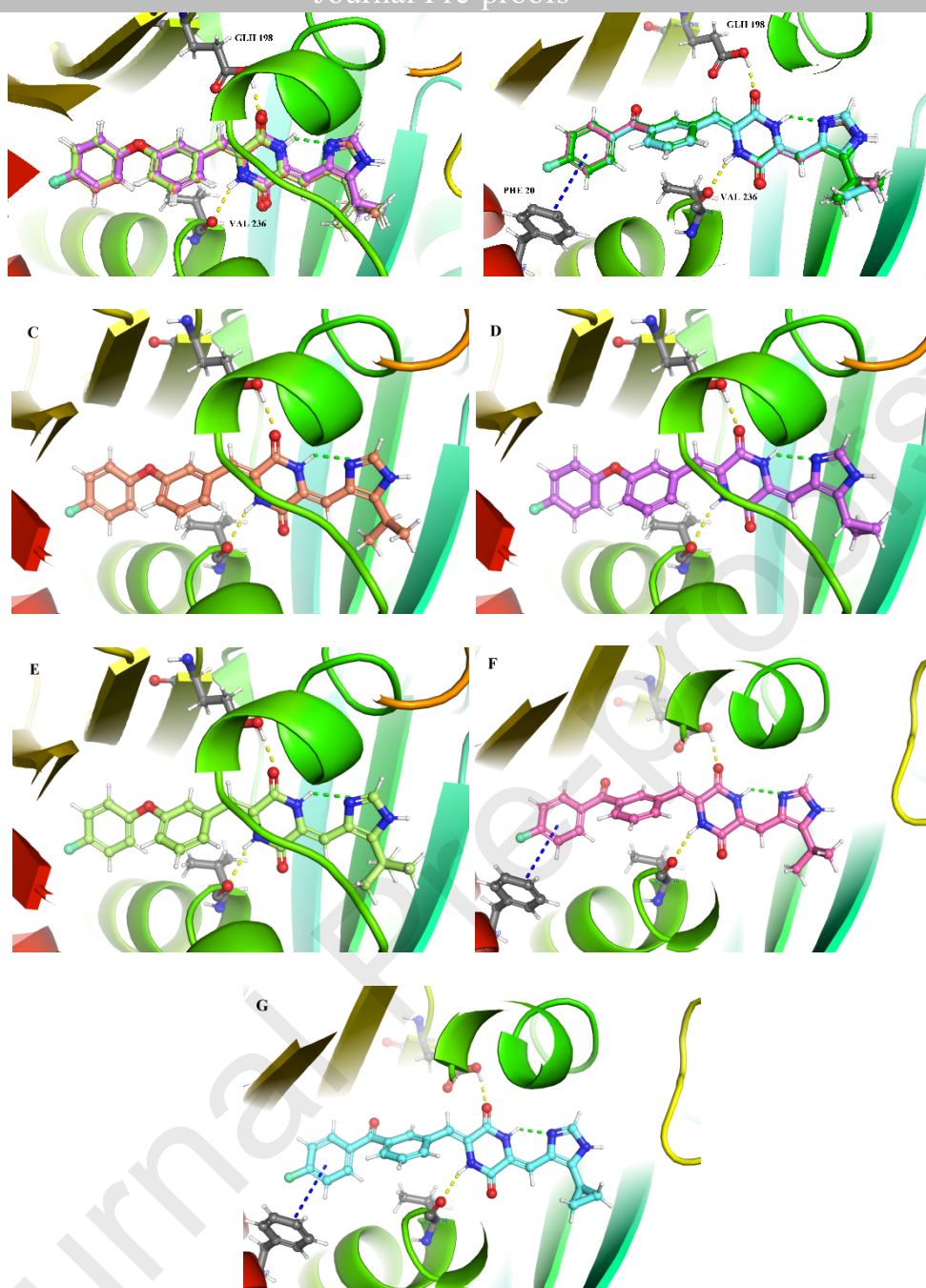


Fig. 6. Binding poses of compounds **1**, compounds **2** and **14a-14d** (stick-model) with co-crystal structure (PDB: 5XHC). A) Compounds **2** (faded-green), **14a** (faded-red-orange) and **14c** (violet) are shown as sticks. B) Compounds **1** (green), **14b** (faded-red) and **14d** (blue) are shown as sticks. C) Compound **14a** (faded-red-orange) are shown as sticks. D) Compound **14c** (violet) are shown as sticks. E) Compound **2** (faded-green) are shown as sticks. F) Compound **14b** (faded-red) are shown as sticks. G) Compound **14d** (blue) are shown as sticks. Yellow dashed: hydrogen bonds of ligand-receptor; green dashed: hydrogen bonds of intra-ligand; blue dashed: π - π interaction.

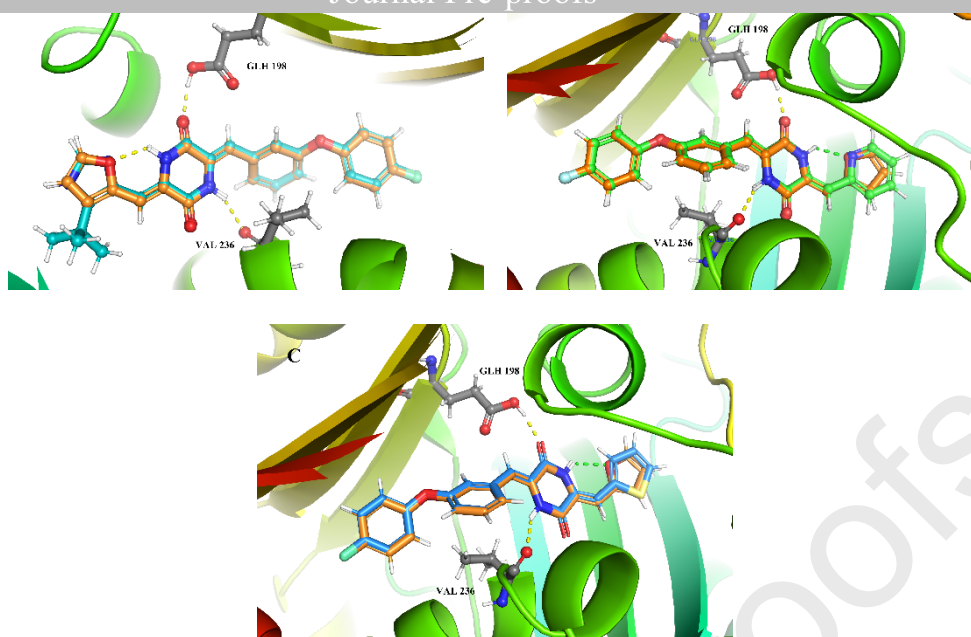


Fig. 7. Binding poses of compounds **2**, **17a**, **17f** and **17g** with co-crystal structure (PDB: 5XHC). A) Compounds **2** (teal), and **17f** (orange) are shown as sticks. B) Compounds **17a** (green) and **17f** (orange) are shown as sticks. C) Compounds **17f** (orange) and **17g** (azure) are shown as sticks. Yellow dashed: hydrogen bonds of ligand-receptor; green dashed: hydrogen bonds of intra-ligand.

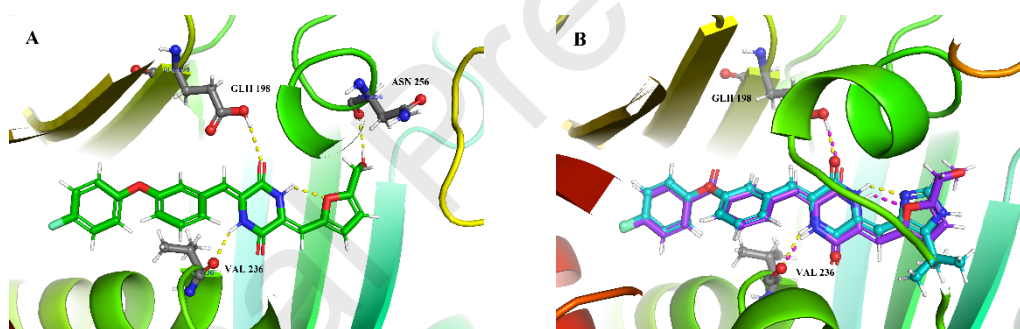


Fig. 8. Binding poses of compounds **1**, **17n** and **17p** with co-crystal structure (PDB: 5XHC). A) **17n** (green) are shown as sticks. B) Compounds **1** (teal) and **17p** (violet) are shown as sticks. Yellow dashed: hydrogen bonds of ligand-receptor; green dashed: hydrogen bonds of intra-ligand.

3. Conclusion

We designed and synthesized a total of 26 novel plinabulin C ring derivatives based on the co-crystal structure of tubulin with compound **1**. Among them, the derivatives **17o** and **17p** with the novel furan group displayed potent cytotoxicity against several human cancer cell lines, which could effectively inhibit tubulin polymerization, as observed in immunofluorescence assay. The docking models of compounds **17o** and **17p** were similar to the co-crystal structure of compound **1**. Based on the SAR study, we found that the appropriate electron-donating group containing the 5-position of furan was important for maintaining the activity of novel furan-diketopiperazine-type derivatives. Therefore, the derivatives **17o** and **17p** with the furan

group could be considered as potential agents in the treatment of cancer. The subsequent pharmaceutical *in vivo* and SAR studies are forthcoming.

4. Experimental section

4.1. General

All starting materials were purchased from commercial suppliers and were used without further purification. Column chromatography was performed on silica gel (200–300 mesh, Yantai Chemical Industry Research Institute). Thin-layer chromatography (TLC) was performed using silica gel GF-254 plates (Qing-Dao Chemical Company, Qingdao, China) with detection by UV (254 nm or 365 nm). Melting points were

(China). ^1H and ^{13}C NMR spectra were obtained using a JEOL 400 spectrometer (400 MHz) or Agilent Pro pulse 500 MHz spectrometer with TMS as an internal standard. The following abbreviations were used to explain the multiplicities: s = singlet, d = doublet, t = triplet, q = quartet, b = broad, td = triple doublet, dt = double triplet, dq = double quartet, and m = multiplet. High-resolution mass spectra (ESI or EI) were recorded on an Agilent 1290 Infinity II UHPLC/6530 Q-TOF mass spectrometer.

4.2. Synthesis

4.2.1. Preparation of ethyl 5-(*tert*-butyl) oxazole-4-carboxylate (**5a**)

To a solution of ethyl isocyanoacetate (100 g, 884.02 mmol) in THF, 1, 8-diazabicyclo[5.4.0]undec-7-ene (DBU) (161.50 g, 1.06 mmol) and pivalic anhydride (197.58 g, 1.06 mmol) were added dropwise. The mixture was stirred for 48 h at room temperature. The reaction solution was removed by evaporation under reduced pressure. The residue was extracted with EtOAc, then washed with 10% Na_2CO_3 and 10% citric acid. The combined organic layer was washed with saturated brine, and dried over anhydrous MgSO_4 . The solvent was concentrated in vacuo, and the crude product was purified by column chromatography (EtOAc–petroleum ether, 4:1) to produce **5a** (172.50 g) as yellow oil with a yield at 99%. ^1H NMR (500 MHz, CDCl_3) δ 7.70 (s, 1H), 4.37 (q, $J = 7.1$ Hz, 2H), 1.45 (s, 9H), 1.40 (t, $J = 7.1$ Hz, 3H). MS (ESI) m/z : $[\text{M} + \text{H}]^+$ Calcd for $\text{C}_{10}\text{H}_{16}\text{NO}_3$: 198.11, Found: 197.82.

4.2.2. Preparation of ethyl 5-(isopropyl) oxazole-4-carboxylate (**5b**)

Ethyl isocyanoacetate (50.00 g, 441.66 mmol), 1, 8-diazabicyclo[5.4.0]undec-7-ene (DBU) (80.69 g, 530.00 mmol) and dimethylacetic anhydride (83.84 g, 530.00 mmol), THF (200 ml), 73 g colourless oil with a yield at 95%. ^1H NMR (500 MHz, CDCl_3) δ 7.73 (s, 1H), 4.37 (q, $J = 7.1$ Hz, 2H), 3.79 (dt, $J = 14.0, 7.0$ Hz, 1H), 1.38 (t, $J = 7.1$ Hz, 3H), 1.28 (d, $J = 7.0$ Hz, 6H). MS (ESI) m/z : $[\text{M} + \text{H}]^+$ Calcd for $\text{C}_9\text{H}_{14}\text{NO}_3$: 184.10, Found: 183.74.

4.2.3. Preparation of ethyl 5-(*tert*-butyl)-1*H*-imidazole-4-carboxylate (**8a**)

A mixture of compound **5a** (27.50 g, 139.43 mmol) and formamide (157.03 g, 485.78 mmol) was heated at 175 °C for 36 h. After cooling, the reaction mixture was added with 10%

extracted with EtOAc. The petroleum ether layer was given up, and the EtOAc layers were combined and washed with saturated brine, and dried over anhydrous MgSO_4 . The solvent was evaporated in vacuo, and the crude product was purified by slurry using H_2O to produce 31.49 g of compound **8a** with a yield at 55%. ^1H NMR (500 MHz, CDCl_3) δ 7.50 (s, 1H), 4.34 (q, $J = 7.1$ Hz, 2H), 1.46 (s, 9H), 1.36 (t, $J = 7.1$ Hz, 3H). MS (ESI) m/z : $[\text{M} + \text{H}]^+$ Calcd for $\text{C}_{10}\text{H}_{17}\text{N}_2\text{O}_2$: 197.13, Found: 196.81.

4.2.4. Preparation of ethyl 5-(isopropyl)-1*H*-imidazole-4-carboxylate (**8b**)

Compound **5b** (5.00 g, 27.29 mmol) and formamide (49.17 g (43 ml), 1.09 mmol), 2.97 g faded orange solid with a yield at 60%. ^1H NMR (500 MHz, CDCl_3) δ 7.60 (s, 1H), 4.31 (q, $J = 7.1$ Hz, 2H), 3.77 (s, 1H), 1.30 (t, 9H). MS (ESI) m/z : $[\text{M} + \text{H}]^+$ Calcd for $\text{C}_9\text{H}_{15}\text{N}_2\text{O}_2$: 183.11, Found: 182.77.

4.2.5. Preparation of ethyl-5-(cyclopropyl)-1*H*-imidazole-4-carboxylate (**8c**)

1) A solution of ethyl 2-cyclopropylacetoacetate (20 g, 128.06 mmol) in CHCl_3 , the mixture was stirred at 0 °C for 10 min, and sulfonyl chloride (20.73 g, 153.66 mmol) was added. The reaction solution was moved to room temperature, stirred for 10 min, and refluxed at 65 °C for 3 h. The solution was extracted with EtOAc, then washed with 10% NaHCO_3 and water. The combined organic layer was washed with saturated brine, and dried over anhydrous sodium sulfate. The solvent was concentrated in vacuo to produce compound **8c** (24 g) as an orange oil with a yield at 97%; this compound was used without further purification.

2) A mixture of ethyl 2-chloro-cyclopropylacetoacetate (67 g, 351.48 mmol), formamide (316 g, 7.03 mol), and water (25 g, 1.40 mmol) was stirred at 145 °C for 20 h. The reaction was monitored by TLC (DCM: MeOH = 20: 1). The mixture was then cooled to room temperature. Then, sodium carbonate aqueous solution was added to separate out a gray solid. The mixture was filtered, and the filter cake was washed with water and dried *in vacuo* at 50 °C to produce 2.90 g of brown solid, with a yield of 4%. ^1H NMR (500 MHz, CDCl_3) δ = 7.54 (s, 1H), 4.37 (d, $J = 7.1$, 2H), 2.65 – 2.53 (m, 1H), 1.38 (t, $J = 7.1$, 3H), 0.99 (d, $J = 7.4$, 4H). MS (ESI) m/z : $[\text{M} + \text{H}]^+$ Calcd for $\text{C}_9\text{H}_{13}\text{N}_2\text{O}_2$: 181.10, Found: 181.35.

methanol (**9a**)

Ethyl 5-(*tert*-butyl)-1*H*-imidazole-4-carboxylate (9.92 g, 261.28 mmol) in THF (80 ml) was added dropwise to a solution of LiAlH₄ (17.07 g, 87.09 mol) in THF (80 mL) at 0 °C under nitrogen. The mixture was stirred for 4 h at room temperature. To this solution, water was added and the resulting precipitate was removed by celite filtration. The filtrate was evaporated *in vacuo* to produce 15.36 g of white solid with a yield of 95 %. The crude product was used in the next step without further purification. MS (ESI) *m/z*: [M + H]⁺ Calcd for C₈H₁₅N₂O: 155.12, Found: 154.64.

4.2.7. Preparation of (5-(isopropyl)-1*H*-imidazol-4-yl) methanol (**9b**)

LiAlH₄ (1.56 g, 41.10 mmol), ethyl 5-(isopropyl)-1*H*-imidazole-4-carboxylate (2.50 g, 13.70 mmol), THF (20 ml), 1.9 g white solid with a yield at 99%. MS (ESI) *m/z*: [M + H]⁺ Calcd for C₇H₁₃N₂O: 141.10, Found: 140.68.

4.2.8. Preparation of (5-(cyclopropyl)-1*H*-imidazol-4-yl) methanol (**9c**)

LiAlH₄ (1.83 g, 48.33 mmol), ethyl 5-(cyclopropyl)-1*H*-imidazole-4-carboxylate (2.90 g, 16.11 mmol), THF (20 ml), 2.09 g orange solid with a yield at 94%. MS (ESI) *m/z*: [M + H]⁺ Calcd for C₇H₁₁N₂O: 139.09, Found: 138.64.

4.2.9. Preparation of 5-(*tert*-butyl)-1*H*-imidazole-4-carbaldehyde (**10a**)

MnO₂ (60.59 g, 696.72 mol) was added to a solution of compound **9a** (13.41 g, 87.09 mmol) in DCM and the mixture was stirred for 48 h at 25 °C. The reaction was monitored by TLC. The solution was filtrated using celite filtration. The solvent was evaporated *in vacuo*, and the crude product was purified by column chromatography (EtOAc–petroleum ether, 4:1) to obtain 9.04 g of white solid with a yield of 68%. ¹H NMR (500 MHz, CDCl₃) δ 10.06 (s, 1H), 7.73 (s, 1H), 1.48 (s, 9H). MS (ESI) *m/z*: [M + H]⁺ Calcd for C₈H₁₃N₂O: 153.10, Found: 152.66.

4.2.10. Preparation of 5-(isopropyl)-1*H*-imidazole-4-carbaldehyde (**10b**)

Compound **9b** (1.92 g, 13.70 mmol), MnO₂ (11.91 g, 0.14 mmol), DCM (20 ml), 1.2 g white solid with a yield at 61%. ¹H NMR (500 MHz, CDCl₃) δ 9.88 (s, 1H), 7.79 (s, 1H), 3.56 – 3.43

for C₇H₁₁N₂O: 139.09, Found: 138.65.

4.2.11. Preparation of 5-(cyclopropyl)-1*H*-imidazole-4-carbaldehyde (**10c**)

Compound **9c** (2.22 g, 16.11 mmol), MnO₂ (13.86 g, 161.11 mmol), DCM (80 ml), 951.2 mg white solid with a yield at 43%. ¹H NMR (400 MHz, CDCl₃) δ 9.87 (s, 1H), 7.74 (s, 1H), 2.27 (s, 1H), 1.09 (d, *J* = 8.3 Hz, 4H). MS (ESI) *m/z*: [M + H]⁺ Calcd for C₇H₉N₂O: 137.07, Found: 136.62.

4.2.12. Preparation of (Z)-1-acetyl-3-((5-(*tert*-butyl)-1*H*-imidazol-4-yl) methylene) piperazine-2, 5-dione (**12a**)

Under nitrogen, a mixture of compound **10a** (4.88 g, 32.11 mmol), 1, 4-diacetylpiperazine-2, 5-dione (12.73 g, 64.21 mmol), and Cs₂CO₃ (15.69 g, 48.16 mmol) in DMF (50 mL) was stirred for 20 h at room temperature. The solution was poured into cool water to precipitate a solid. The mixture was filtered to produce 4.43 g of orange solid with a yield of 47 %. ¹H NMR (500 MHz, DMSO-*d*₆) δ 12.36 (s, 1H), 12.01 (s, 1H), 7.85 (s, 1H), 7.04 (s, 1H), 4.30 (s, 2H), 2.49 (s, 3H), 1.39 (s, 9H). MS (ESI) *m/z*: [M + H]⁺ Calcd for C₁₄H₁₉N₄O₃: 291.15, Found: 290.79.

4.2.13. Preparation of (Z)-1-acetyl-3-((5-(isopropyl)-1*H*-imidazol-4-yl) methylene) piperazine-2, 5-dione (**12b**)

Compound **10b** (500.00 mg, 3.70 mmol), 1, 4-diacetylpiperazine-2, 5-dione (1.47 g, 7.40 mmol) and Cs₂CO₃ (1.81 g, 5.55 mmol), DMF (4 mL). 367.0 mg orange solid with a yield at 36%. ¹H NMR (500 MHz, DMSO-*d*₆) δ 12.60 (s, 1H), 11.78 (s, 1H), 7.90 (s, 1H), 6.80 (s, 1H), 4.31 (s, 2H), 3.30 – 3.16 (m, 1H), 2.50 (d, *J* = 3.9 Hz, 3H), 1.24 (d, *J* = 6.9 Hz, 6H). MS (ESI) *m/z*: [M + H]⁺ Calcd for C₁₃H₁₇N₄O₃: 277.13, Found: 276.83.

4.2.14. Preparation of (Z)-1-acetyl-3-((5-(cyclopropyl)-1*H*-imidazol-4-yl) methylene) piperazine-2, 5-dione (**12c**)

Compound **10c** (1.53 g, 11.24 mmol), 1, 4-diacetylpiperazine-2, 5-dione (4.45 g, 22.48 mmol) and Cs₂CO₃ (1.81 g, 5.55 mmol), DMF (15 mL). 1.2 g orange solid with a yield at 39%. ¹H NMR (500 MHz, DMSO-*d*₆) δ 12.34 (s, 1H), 11.69 (s, 1H), 7.81 (s, 1H), 6.88 (s, 1H), 4.30 (s, 2H), 2.49 (s, 3H), 2.15 – 1.94 (m, 1H), 1.07 – 0.91 (m, 2H), 0.76 (t, *J* = 3.2 Hz, 2H). MS (ESI) *m/z*: [M + H]⁺ Calcd for C₁₃H₁₅N₄O₃: 275.11, Found: 274.78.

4.2.15. Preparation of (Z)-1-acetyl-3-((5-(methyl)-1*H*-imidazol-4-yl) methylene-*d*) piperazine-2, 5-dione (**12d**)

diacetylpiperazine-2, 5-dione (13.60 g, 18.16 mmol) and Cs_2CO_3 (4.44 g, 13.62 mmol), DMF (18 mL). 1.06 g orange solid with a yield at 47%. ^1H NMR (500 MHz, $\text{DMSO-}d_6$) δ 12.56 (s, 1H), 11.74 (s, 1H), 7.87 (s, 1H), 6.76 (s, 1H), 4.31 (s, 2H), 2.50 (s, 3H), 2.33 (s, 3H). MS (ESI) m/z : $[\text{M} + \text{H}]^+$ Calcd for $\text{C}_{11}\text{H}_{13}\text{N}_4\text{O}_3$: 249.10, Found: 248.81.

4.2.16. Preparation of (Z)-1-acetyl-3-((1H-imidazol-4-yl)methylene-d) piperazine-2, 5-dione (**12e**)

Compound **10e** (1.00 g, 10.41 mmol), 1, 4-diacetylpiperazine-2, 5-dione (4.13 g, 20.82 mmol) and Cs_2CO_3 (5.09 g, 15.62 mmol), DMF (10 mL). 1.0 g orange solid with a yield at 41%. ^1H NMR (500 MHz, $\text{DMSO-}d_6$) δ 12.68 (s, 1H), 11.70 (s, 1H), 7.99 (s, 1H), 7.63 (s, 1H), 6.83 (s, 1H), 4.32 (s, 2H), 2.57 – 2.37 (s, 3H). MS (ESI) m/z : $[\text{M} + \text{H}]^+$ Calcd for $\text{C}_{10}\text{H}_{11}\text{N}_4\text{O}_3$: 235.08, Found: 234.79.

4.2.17. Preparation of 3-(4-fluorobenzoyl) benzaldehyde (**13a**)

To a solution of 4-fluorophenol (500 mg, 4.46 mol) in dry DCM (10 mL), (3-formylphenyl)boronic acid (1.00 g, 6.69 mol), $\text{Cu}(\text{OAc})_2$ (811 mg, 4.46 mol) and Et_3N (135.6 mg, 1.34 mol) were added under O_2 atmosphere and the mixture was stirred at 25°C for 48 h. The mixture was diluted with brine and extracted with EtOAc. The solvent was removed under reduced pressure. The residue was purified by silica gel column chromatography using petroleum ether/ethyl acetate (10:1) to produce 0.22 g of 0.22 g with a yield of 22%.

^1H NMR (500 MHz, CDCl_3) δ 9.96 (s, 1H), 7.59 (d, $J = 7.5$ Hz, 1H), 7.50 (t, $J = 7.8$ Hz, 1H), 7.41 (dd, $J = 2.2, 1.4$ Hz, 1H), 7.25 (dt, $J = 3.5, 1.4$ Hz, 1H), 7.10 – 7.04 (m, 2H), 7.02 (ddd, $J = 6.8, 5.2, 3.0$ Hz, 2H). MS (ESI) m/z : $[\text{M} + \text{H}]^+$ Calcd for $\text{C}_{13}\text{H}_{10}\text{FO}_2$: 217.07, Found: 217.27.

4.2.18. Preparation of 3-(4-fluorophenoxy) benzaldehyde (**13b**)

The tetrahydrofuran solution (12 mL) of 2-(3-bromophenyl)-1, 3-dioxolane (4.88 g, 21.29 mmol) was added dropwise to a solution of *n*-BuLi (20.48 ml (1.6 M THF)), 32.75 mmol) in dry THF (20 mL) at -78°C under nitrogen atmosphere. The solution was then stirred at -78°C under nitrogen atmosphere for 50 min. A solution of 4-fluoro-N-methyl-N-methoxybenzamide (3.0 g, 16.38 mmol) in THF (10 ml) was

The reaction mixture was quenched using a saturated ammonium chloride solution. The residue was dissolved in methanol and hydrochloric acid (2 mol/L) was added. The mixture was stirred at room temperature. The solvent was moved under pressure, extracted with EtOAc (100 ml * 3), washed with saturated NaCl (50 ml * 3), dried over anhydrous sodium sulfate, and concentrated in vacuo. The residue was purified by silica gel column chromatography using petroleum ether/ethyl acetate (10:1/8:1) to produce 2.51 g of white solid with a yield of 67%. ^1H NMR (500 MHz, $\text{DMSO-}d_6$) δ 10.11 (s, 1H), 8.24 – 8.18 (m, 2H), 8.07 – 8.03 (m, 1H), 7.90 – 7.85 (m, 2H), 7.80 (t, $J = 7.7$ Hz, 1H), 7.46 – 7.39 (m, 2H). MS (ESI) m/z : $[\text{M} + \text{H}]^+$ Calcd for $\text{C}_{14}\text{H}_{10}\text{FO}_2$: 229.07, Found: 228.75.

4.2.19. Preparation of (Z)-N-acetyl-3-(4-fluorobenzoyl)benzylidene) piperazine-2, 5-dione (**15a**)

A mixture of 3-*para*-fluorophenoxybenzaldehyde (156.77 mg, 0.72 mmol), 1, 4-diacetylpiperazine-2, 5-dione (150 mg, 0.60 mmol), cesium carbonate (295.32 mg, 0.91 mmol), and anhydrous sodium sulfate (171.66 mg, 1.21 mmol) was stirred in DMF (3 mL) under nitrogen at room temperature for 20 h. The reaction was detected by thin-layer chromatography. The reaction solution was poured into cold water. The mixture solution was filtered, then the filter cake was washed with water and dried in vacuum drying equipment at 50 °C to obtain 115.0 mg of faded-orange solid with a yield of 47 %. The product was directly used in the next reaction without further purification. ^1H NMR (500 MHz, $\text{DMSO-}d_6$) δ 10.41 (s, 1H), 7.43 (t, $J = 7.9$ Hz, 1H), 7.32 (d, $J = 8.1$ Hz, 1H), 7.27 – 7.20 (m, 3H), 7.11 (ddd, $J = 6.8, 5.4, 3.2$ Hz, 2H), 6.96 – 6.91 (m, 2H), 4.35 (s, 2H), 2.49 (s, 3H). MS (ESI) m/z : $[\text{M} + \text{H}]^+$ Calcd for $\text{C}_{19}\text{H}_{16}\text{FN}_2\text{O}_4$: 355.11, Found: 354.90.

4.2.20. Preparation of (Z)-N-acetyl-3-(4-fluorophenoxy)benzylidene) piperazine-2, 5-dione (**15b**)

3-*para*-fluorobenzoylbenzaldehyde (1.06 g, 4.63 mmol), 1, 4-diacetylpiperazine-2, 5-dione (1.83 g, 9.25 mmol), Cs_2CO_3 (2.01 g, 6.94 mmol), Na_2SO_4 (1.31 g, 9.25 mmol), DMF (15 mL), 1.3 g faded-orange solid with a yield at 77%. ^1H NMR (500 MHz, $\text{DMSO-}d_6$) δ 10.53 (s, 1H), 7.94 – 7.88 (m, 3H), 7.81 (d, $J = 7.7$ Hz, 1H), 7.68 (d, $J = 7.8$ Hz, 1H), 7.61 (t, $J = 7.7$ Hz, 1H), 7.40 (dd, $J = 12.3, 5.4$ Hz, 2H), 7.02 (s, 1H), 4.36 (s, 2H), 2.50 (s, 3H). MS (ESI) m/z : $[\text{M} + \text{H}]^+$ Calcd for $\text{C}_{20}\text{H}_{16}\text{FN}_2\text{O}_4$: 367.11, Found: 366.93.

methyl) furan-2-carbaldehyde (**16a**)

A mixture of 5-hydroxymethylfurfural (1.26 g, 10.00 mmol), potassium carbonate (748.88 mg, 11.00 mmol), and *tert*-butyldimethylchlorosilane (1.66 g, 11.00 mmol) was stirred in DCM at room temperature for 12 h. The reaction solution was filtered using silica gel and washed with petroleum ether. The solvent was removed under reduced pressure to obtain 2.4 g of brown oil with a yield of 99%. ¹H NMR (500 MHz, DMSO-*d*₆) δ 9.56 (s, 1H), 7.49 (d, *J* = 3.5 Hz, 1H), 6.63 (d, *J* = 3.6 Hz, 1H), 4.73 (s, 2H), 0.87 (s, 9H), 0.08 (s, 6H). MS (ESI) *m/z*: [M + H]⁺ Calcd for C₁₂H₂₁O₃Si: 241.13, Found: 240.85.

4.2.22. Preparation of 5-(methoxymethyl) furan-2-carbaldehyde (**16b**)

A mixture of 5-hydroxymethylfurfural (500.00 mg, 3.96 mmol), methyl iodide (1.69 g, 11.89 mmol), and cesium carbonate (1.94 g, 5.95 mmol) was stirred in acetonitrile (20 ml) at 50 °C for 24 h. The reaction was monitored by LC-MS. The residue was purified by silica gel column chromatography using ethyl acetate/petroleum ether (1: 20, 1:15, 1:10, 1: 8, 1: 5) to produce 280.0 mg of yellow liquid with a yield of 50%. ¹H NMR (500 MHz, DMSO-*d*₆) δ 9.58 (s, 1H), 7.51 (d, *J* = 3.5 Hz, 1H), 6.73 (d, *J* = 3.6 Hz, 1H), 4.47 (s, 2H), 3.30 (s, 3H). MS (ESI) *m/z*: [M + H]⁺ Calcd for C₇H₉O₃: 141.05, Found: 140.88.

General procedure for synthesis of **1**, **2** and **14a-14h**, and synthesis of **14a** as an example.

A mixture of (*Z*)-1-acetyl-3-((5-(isopropyl)-1H-imidazol-4-yl) methylene) piperazine-2, 5-dione (211.83 mg, 0.77 mmol), 3-(4-fluorobenzoyloxy) benzaldehyde (150.0 mg, 0.69 mmol), Cs₂CO₃ (282.55 mg, 0.87 mmol), and Na₂SO₄ (164.23 mg, 1.16 mmol) was stirred in DMF (4 ml) under nitrogen at 60 °C for 24 h. The resulting solution was poured into cold water (40 ml) and the filter cake was re-dissolved using methanol and dichloromethane (1:3) then filtered. The solvent was combined and concentrated under reduced pressure. The filtrate was stirred in methanol at room temperature for 2 h, then moved to 0 °C. The solution was filtered, washed with methanol, and dried *in vacuo* at 50 °C to produce 231.4 mg of yellow solid with a yield of 70 %.

4.2.23. (3*Z*, 6*Z*)-3-(4-fluorophenoxy) benzylidene)-6-((5-(*tert*-butyl)-1H-imidazol-4-yl) methylene)- piperazine-2, 5-dione (**2**)

Cs₂CO₃ (531.00 mg, 1.63 mmol), 300 mg yellow solid with a yield at 64%. MP: 260-262°C. ¹H NMR (500 MHz, DMSO-*d*₆) δ 12.29 (d, *J* = 33.1 Hz, 2H), 10.10 (s, 1H), 7.85 (s, 1H), 7.41 (t, *J* = 7.9 Hz, 1H), 7.31-7.07 (m, 6H), 6.90 (d, *J* = 8.1 Hz, 1H), 6.86 (s, 1H), 6.71 (s, 1H), 1.38 (s, 9H). ¹³C NMR (125 MHz, DMSO-*d*₆) δ 159.1, 157.5, 157.2, 156.9 (*J*_{C-F} = 113.1 Hz), 152.6, 140.4, 135.2, 134.4, 130.7, 130.3, 127.3, 124.4, 123.7, 120.5*2 (*J*_{C-F} = 8.5 Hz), 118.9, 117.7, 116.5*2 (*J*_{C-F} = 23.2 Hz), 113.0, 105.2, 31.9, 30.6*3. MS (ESI) *m/z*: [M + H]⁺ Calcd for C₂₅H₂₄FN₄O₃: 447.1827, Found: 447.18.

4.2.24. (3*Z*, 6*Z*)-3-(4-fluorobenzoyl) benzylidene)-6-((5-(*tert*-butyl)-1H-imidazol-4-yl) methylene)- piperazine-2, 5-dione (**1**)

12a (200.00 mg, 0.69 mmol), **13b** (188.67 mg, 0.83 mmol), Cs₂CO₃ (336.67 mg, 1.03 mmol), 221.4 mg yellow solid with a yield at 70%. MP: 255-257°C. ¹H NMR (400 MHz, DMSO-*d*₆) δ 12.33 (s, 1H), 12.29 (s, 1H), 10.34 (s, 1H), 7.95-7.88 (m, 2H), 7.85 (s, 1H), 7.82 (s, 1H), 7.75 (d, *J* = 7.55 Hz, 1H), 7.64 (d, *J* = 7.70 Hz, 1H), 7.58 (t, *J* = 7.58 Hz, 1H), 7.40 (t, *J* = 8.82 Hz, 2H), 6.86 (s, 1H), 6.80 (s, 1H), 1.38 (s, 9H). MS (ESI) *m/z*: [M + H]⁺ Calcd for C₂₆H₂₄FN₄O₃: 459.1827, Found 459.15.

4.2.25. (3*Z*, 6*Z*)-3-(4-fluorophenoxy) benzylidene)-6-((5-(isopropyl)-1H-imidazol-4-yl) methylene)- piperazine-2, 5-dione (**14a**)

12b (211.83 mg, 0.77 mmol), **13a** (150.00 mg, 0.69 mmol), Cs₂CO₃ (282.55 mg, 0.87 mmol), Na₂SO₄ (164.23 mg, 1.16 mmol), 231.4 mg yellow solid with a yield at 70%. MP: 246-248°C. ¹H NMR (500 MHz, DMSO-*d*₆) δ 12.58 (s, 1H), 12.02 (s, 1H), 10.12 (s, 1H), 7.90 (s, 1H), 7.40 (t, *J* = 7.9 Hz, 1H), 7.24 (m, 3H), 7.17 (s, 1H), 7.14 - 7.09 (m, 2H), 6.90 (dd, *J* = 8.2, 2.1 Hz, 1H), 6.71 (s, 1H), 6.61 (s, 1H), 3.25 (dt, *J* = 13.9, 6.9 Hz, 1H), 1.23 (d, *J* = 6.9 Hz, 6H). ¹³C NMR (125 MHz, DMSO-*d*₆) δ 159.14, 157.43, 157.08, 156.11, 152.58, 139.02, 135.33, 135.22, 130.70, 130.29, 127.33, 124.39, 123.68, 120.57*2 (*J*_{C-F} = 8.5 Hz), 118.85, 117.71, 116.54*2 (*J*_{C-F} = 23.3 Hz), 113.00, 104.02, 24.00, 22.53*2. HRMS (ESI) *m/z*: [M + H]⁺ Calcd for C₂₄H₂₂FN₄O₃: 433.1670, Found 433.1673.

4.2.26. (3*Z*, 6*Z*)-3-(4-fluorobenzoyl) benzylidene)-6-((5-(isopropyl)-1H-imidazol-4-yl) methylene)- piperazine-2, 5-dione (**14b**)

Cs₂CO₃ (353.78 mg, 1.09 mmol), Na₂SO₄ (205.63 mg, 1.45 mmol), DMF (4 ml), 115.6 mg yellow solid with a yield at 36%. MP: 156-157°C. ¹H NMR (500 MHz, DMSO-*d*₆) δ 12.56 (s, 1H), 12.01 (s, 1H), 10.37 (s, 1H), 7.90 (m, 3H), 7.83 (s, 1H), 7.77 (d, *J* = 7.1, 1H), 7.62 (d, *J* = 7.1 Hz, 1H), 7.60-7.53 (m, 1H), 7.40 (t, *J* = 8.6, 2H), 6.78 (s, 1H), 6.60 (s, 1H), 3.27-3.22 (m, 1H), 1.23 (d, *J* = 6.6, 6H). ¹³C NMR (125 MHz, DMSO-*d*₆) δ 194.18, 165.74, 163.74, 157.57, 156.03, 139.03, 137.28, 135.33, 133.57, 133.32, 132.78*2 (*J*_{C-F} = 9.4 Hz), 130.69, 130.10, 128.85, 128.68, 127.76, 123.70, 115.70*2 (*J*_{C-F} = 21.9 Hz), 112.59, 104.04, 23.98, 22.52*2. HRMS (ESI) *m/z*: [M + H]⁺ Calcd for C₂₅H₂₂FN₄O₃: 445.1670, Found: 445.1672.

4.2.27. (3*Z*, 6*Z*)-3-(4-fluorophenoxy) benzylidene)-6-((5-(cyclopropyl)-1*H*-imidazol-4-yl) methylene)- piperazine-2, 5-dione (**14c**)

12c (150.00 mg, 0.55 mmol), **13a** (141.90 mg, 0.66 mmol), Cs₂CO₃ (267.27 mg, 0.42 mmol), Na₂SO₄ (155.36 mg, 1.09 mmol), DMF (3 ml), 101.1 mg yellow solid with a yield at 43%. MP: 257-259°C. ¹H NMR (500 MHz, DMSO-*d*₆) δ 12.31 (s, 1H), 11.94 (s, 1H), 10.12 (s, 1H), 7.82 (s, 1H), 7.41 (t, *J* = 7.9 Hz, 1H), 7.29 – 7.20 (m, 3H), 7.17 (s, 1H), 7.14 – 7.08 (m, 2H), 6.90 (dd, *J* = 8.2, 2.2 Hz, 1H), 6.72 (s, 2H), 2.14 – 2.06 (m, 1H), 1.04 – 0.95 (m, 2H), 0.80 – 0.73 (m, 2H). ¹³C NMR (125 MHz, DMSO-*d*₆) δ 159.13, 157.39, 157.06, 156.08, 152.59, 135.22, 135.05, 134.88, 133.09, 130.28, 127.33, 124.38, 123.54, 120.55*2 (*J*_{C-F} = 8.5 Hz), 118.86, 117.70, 116.53*2 (*J*_{C-F} = 23.3 Hz), 112.94, 104.18, 7.38*2, 5.43. HRMS (ESI) *m/z*: [M + H]⁺ Calcd for C₂₄H₂₀FN₄O₃: 431.1514, Found 431.1514.

4.2.28. (3*Z*, 6*Z*)-3-(4-fluorobenzoyl) benzylidene)-6-((5-(cyclopropyl)-1*H*-imidazol-4-yl) methylene)- piperazine-2, 5-dione (**14d**)

12c (70.00 mg, 0.26 mmol), **13b** (69.90 mg, 0.31 mmol), Cs₂CO₃ (124.72 mg, 0.38 mmol), Na₂SO₄ (72.50 mg, 0.51 mmol), DMF (3 ml), 79.5 mg yellow solid with a yield at 70%. MP: 217-219°C. ¹H NMR (500 MHz, DMSO-*d*₆) δ 12.30 (s, 1H), 11.95 (s, 1H), 10.30 (s, 1H), 7.96–7.87 (m, 2H), 7.81 (s, 2H), 7.75 (d, *J* = 7.21 Hz, 1H), 7.67–7.53 (m, 2H), 7.40 (t, *J* = 8.49 Hz, 2H), 6.80 (s, 1H), 6.71 (s, 1H), 2.10 (s, 1H), 0.99 (d, *J* = 7.05 Hz, 2H), 0.77 (d, *J* = 4.08 Hz, 2H). ¹³C NMR (125 MHz, DMSO-*d*₆) δ 194.17, 165.74, 163.74, 157.54, 156.01, 137.28, 135.08, 134.88, 133.56, 133.32, 132.78*2 (*J*_{C-F} = 9.4 Hz), 130.10, 128.86, 128.68, 127.75, 123.56, 115.70*2 (*J*_{C-F} = 21.9 Hz), 112.57, 104.22, 7.39*2, 5.43.

465.1339, Found 465.1328.

4.2.29. (3*Z*, 6*Z*)-3-(4-fluorophenoxy) benzylidene)-6-((5-(methyl)-1*H*-imidazol-4-yl) methylene)- piperazine-2, 5-dione (**14e**)

12d (150.00 mg, 0.60 mmol), **13a** (156.77 mg, 0.73 mmol), Cs₂CO₃ (295.32 mg, 0.91 mmol), Na₂SO₄ (171.66 mg, 1.21 mmol), DMF (2 ml), 115.0 mg yellow solid with a yield at 47%. MP: 219-221°C. ¹H NMR (500 MHz, DMSO-*d*₆) δ 12.54 (s, 1H), 11.99 (s, 1H), 10.11 (s, 1H), 7.87 (s, 1H), 7.41 (t, *J* = 7.9 Hz, 1H), 7.29 – 7.21 (m, 3H), 7.17 (s, 1H), 7.14 – 7.10 (m, 2H), 6.90 (dd, *J* = 8.2, 2.2 Hz, 1H), 6.71 (s, 1H), 6.59 (s, 1H), 2.32 (s, 3H). ¹³C NMR (125 MHz, DMSO-*d*₆) δ 159.15, 157.41, 157.09, 156.10, 152.59, 135.22, 135.12, 132.48, 130.30, 129.16, 127.34, 124.39, 123.48, 120.58*2 (*J*_{C-F} = 8.5 Hz), 118.85, 117.71, 116.55*2 (*J*_{C-F} = 23.3 Hz), 112.96, 104.19, 9.05. HRMS (ESI) *m/z*: [M + H]⁺ Calcd for C₂₂H₁₈FN₄O₃: 405.1357, Found 405.1351.

4.2.30. (3*Z*, 6*Z*)-3-(4-fluorobenzoyl) benzylidene)-6-((5-(methyl)-1*H*-imidazol-4-yl) methylene)- piperazine-2, 5-dione (**14f**)

12d (200.00 mg, 0.81 mmol), **13b** (220.64 mg, 0.97 mmol), Cs₂CO₃ (393.77 mg, 1.21 mmol), DMF (3 ml), 96.25 mg yellow solid with a yield at 29%. MP: 243-245°C. ¹H NMR (500 MHz, DMSO-*d*₆) δ 12.52 (s, 1H), 12.00 (s, 1H), 10.30 (s, 1H), 7.91 (dd, *J* = 5.65, 8.44 Hz, 2H), 7.87 (s, 1H), 7.82 (s, 1H), 7.75 (d, *J* = 7.62 Hz, 1H), 7.64 (d, *J* = 7.70 Hz, 1H), 7.58 (t, *J* = 7.63 Hz, 1H), 7.40 (t, *J* = 8.72 Hz, 2H), 6.80 (s, 1H), 6.60 (s, 1H), 2.32 (s, 3H). ¹³C NMR (125 MHz, DMSO-*d*₆) δ 194.18, 165.74, 163.74, 157.55, 156.02, 137.28, 135.11, 133.56, 133.32, 132.78*2 (*J*_{C-F} = 9.4 Hz), 132.47, 130.11, 129.16, 128.86, 128.68, 127.76, 123.49, 115.70*2 (*J*_{C-F} = 21.9 Hz), 112.56, 104.22, 9.04. HRMS (ESI) *m/z*: [M + Na]⁺ Calcd for C₂₃H₁₇FN₄O₃Na: 439.1182, Found: 439.1181.

4.2.31. (3*Z*, 6*Z*)-3-(4-fluorophenoxy) benzylidene)-6-((1*H*-imidazol-4-yl) methylene)- piperazine-2, 5-dione (**14g**)

12e (150.00 mg, 0.64 mmol), **13a** (166.16 mg, 0.77 mmol), Cs₂CO₃ (312.98 mg, 0.96 mmol), Na₂SO₄ (181.93 mg, 1.28 mmol), DMF (3 ml), 56.9 mg yellow solid with a yield at 23%. MP: 202-204°C. ¹H NMR (500 MHz, DMSO-*d*₆) δ 12.65 (s, 1H), 11.90 (s, 1H), 10.14 (s, 1H), 7.99 (s, 1H), 7.58 (s, 1H), 7.40 (t, *J* = 7.9 Hz, 1H), 7.27 (d, *J* = 8.0 Hz, 1H), 7.25 – 7.20 (m, 2H), 7.17 (s, 1H), 7.14 – 7.07 (m, 2H), 6.90 (dd, *J* = 8.2, 2.3 Hz, 1H), 6.72

157.32, 157.07, 156.17, 152.57, 136.64, 136.38, 135.19, 130.29, 127.25, 124.49, 124.39, 120.55*2 ($J_{C-F} = 8.5$ Hz), 119.71, 118.90, 117.75, 116.53*2 ($J_{C-F} = 23.3$ Hz), 113.20, 105.27. HRMS (ESI) m/z : $[M + H]^+$ Calcd for $C_{21}H_{16}FN_4O_3$: 391.1201, Found 391.1194.

4.2.32. (3Z, 6Z)-3-(4-fluorobenzoyl) benzylidene-6-((1H-imidazol-4-yl) methylene)- piperazine-2, 5-dione (**14h**)

12e (150.00 mg, 0.64 mmol), **13b** (141.42 mg, 0.77 mmol), Cs_2CO_3 (312.98 mg, 0.96 mmol), Na_2SO_4 (181.93 mg, 1.28 mmol), DMF (3 ml), 115.9 mg yellow solid with a yield a 45%. MP: 150-152°C. 1H NMR (500 MHz, $DMSO-d_6$) δ 12.67 (s, 1H), 11.92 (s, 1H), 10.36 (s, 1H), 8.00 (s, 1H), 7.95 – 7.87 (m, 2H), 7.82 (s, 1H), 7.75 (d, $J = 7.7$ Hz, 1H), 7.64 (d, $J = 7.7$ Hz, 1H), 7.58 (dd, $J = 8.9, 6.3$ Hz, 2H), 7.40 (t, $J = 8.8$ Hz, 2H), 6.81 (s, 1H), 6.67 (s, 1H). ^{13}C NMR (125 MHz, $DMSO-d_6$) δ 194.17, 165.74, 163.74, 157.47, 156.10, 137.29, 136.65, 136.38, 133.54, 133.32, 132.78*2 ($J_{C-F} = 9.4$ Hz), 130.14, 128.87, 128.72, 127.68, 124.51, 119.73, 115.70*2 ($J_{C-F} = 22.0$ Hz), 112.84, 105.32. HRMS (ESI) m/z : $[M + Na]^+$ Calcd for $C_{22}H_{15}FN_4O_3Na$: 425.1026, Found 425.1026.

General procedure for synthesis of **17a-17m** and **17o-17r**, and synthesis of **17a** as an example.

A mixture of (Z)-N-acetyl-3-((3-*para*-fluorophenoxyphenyl) methylene) piperazine-2, 5-dione **15a** (100 mg, 0.28 mmol), 2-pyridinaldehyde (45.34 mg, 0.42 mmol), cesium carbonate (137.9 mg, 0.42 mmol), and anhydrous sodium sulfate (80.2 mg, 0.56 mmol), was stirred in DMF (3 ml) under nitrogen at 45°C for 24 h. The resulting solution was dropped into cold water (4°C, 60 ml), then filtered, and the filter cake was washed with cold water, then dried *in vacuo* at 50 °C. The filtration was stirred in methanol at room temperature for 2 h, then moved to 0 °C. The solution was filtered, washed with methanol, and dried in vacuum at 50°C to obtain 80.8 mg of yellow solid with a yield of 71%.

4.2.33. (3Z, 6Z)-3-(4-fluorophenoxy) benzylidene-6-(2-pyridylmethylene) piperazine-2, 5-dione (**17a**)

15a (100.00 mg, 0.28 mmol), 2-pyridinaldehyde (45.34 mg, 0.42 mmol), Cs_2CO_3 (137.90 mg, 0.42 mmol), Na_2SO_4 (80.20 mg, 0.56 mmol), DMF (3 ml), 80.8 mg yellow solid with a yield at 71%. MP: 198-200°C. 1H NMR (500 MHz, $DMSO-d_6$) δ 12.59 (s, 1H), 10.48 (s, 1H), 8.73 (t, $J = 5.9$ Hz, 1H), 7.91 (td, $J = 7.8, 1.8$ Hz, 1H), 7.68 (d, $J = 8.0$ Hz, 1H), 7.42 (t, $J = 7.9$ Hz, 1H),

7.26 – 7.19 (m, 3H), 7.15 – 7.10 (m, 2H), 6.92 (dd, $J = 8.1, 2.0$ Hz, 1H), 6.81 (s, 1H), 6.72 (s, 1H). ^{13}C NMR (125 MHz, $DMSO-d_6$) δ 159.14, 157.24, 157.05, 156.72, 156.66, 154.60, 152.56, 148.52, 137.76, 134.87, 131.00, 130.29, 126.70, 126.53, 124.61, 122.54, 120.56 ($J_{C-F} = 8.4$ Hz), 119.07, 118.03, 116.53 ($J_{C-F} = 23.3$ Hz), 114.78, 107.73. HRMS (ESI) m/z : $[M + H]^+$ Calcd for $C_{23}H_{17}FN_3O_3$: 402.1248, Found 402.1249.

4.2.34. (3Z, 6Z)-3-(4-fluorophenoxy) benzylidene-6-(3-pyridylmethylene) piperazine-2, 5-dione (**17b**)

15a (100.00 mg, 0.28 mmol), 3-pyridinaldehyde (45.34 mg, 0.42 mmol), Cs_2CO_3 (137.90 mg, 0.42 mmol), Na_2SO_4 (80.20 mg, 0.56 mmol), DMF (3 ml), 84.2 mg yellow solid with a yield at 74%. MP: 263-266°C. 1H NMR (500 MHz, $DMSO-d_6$) δ 10.68 (s, 1H), 10.42 (s, 1H), 8.69 (s, 1H), 8.48 (s, 1H), 7.93 (d, $J = 7.1$ Hz, 1H), 7.42 (d, $J = 7.0$ Hz, 2H), 7.32 – 7.18 (m, 4H), 7.13 (s, 2H), 6.92 (d, $J = 7.0$ Hz, 1H), 6.76 (s, 2H). ^{13}C NMR (125 MHz, $DMSO-d_6$) δ 159.20, 157.97, 157.65, 157.04, 152.53, 150.17, 148.44, 136.18, 135.02, 130.27, 128.11, 127.36, 127.08, 124.53, 123.49, 120.56 ($J_{C-F} = 8.5$ Hz), 118.91, 117.93, 116.54 ($J_{C-F} = 23.3$ Hz), 114.38, 111.39. HRMS (ESI) m/z : $[M + H]^+$ Calcd for $C_{23}H_{17}FN_3O_3$: 402.1248, Found 402.1243.

4.2.35. (3Z, 6Z)-3-(4-fluorophenoxy) benzylidene-6-(benzylidene) piperazine-2, 5-dione (**17c**)

15a (100.00 mg, 0.28 mmol), benzaldehyde (44.92 mg, 0.42 mmol), Cs_2CO_3 (137.90 mg, 0.42 mmol), Na_2SO_4 (80.20 mg, 0.56 mmol), DMF (3 ml), 67.4 mg yellow solid with a yield at 60%. MP: 275-277°C. 1H NMR (500 MHz, $DMSO-d_6$) δ 10.32 (d, $J = 26.6$ Hz, 2H), 7.54 (s, 2H), 7.42 (s, 3H), 7.34 – 7.08 (m, 7H), 6.92 (s, 1H), 6.76 (d, 2H). ^{13}C NMR (125 MHz, $DMSO-d_6$) δ 158.00, 157.03, 135.07, 133.05, 130.27, 129.33*2, 128.67*2, 128.19, 126.31, 124.51, 120.59, 120.52, 118.92, 117.90, 116.63, 116.45, 115.13, 114.14. HRMS (ESI) m/z : $[M + H]^+$ Calcd for $C_{24}H_{18}FN_2O_3$: 401.1296, Found 401.1294.

4.2.36. (3Z, 6Z)-3-(4-fluorophenoxy) benzylidene-6-(cyclohexylmethylene) piperazine-2, 5-dione (**17d**)

15a (100.00 mg, 0.28 mmol), cyclohexane formaldehyde (47.48 mg, 0.42 mmol), Cs_2CO_3 (137.90 mg, 0.42 mmol), Na_2SO_4 (80.20 mg, 0.56 mmol), DMF (3 ml), 13.8 mg yellow solid with a yield at 12%. MP: 227-229°C. 1H NMR (400 MHz, $DMSO-d_6$) δ 10.43 (s, 1H), 10.11 (s, 1H), 7.39 (t, $J = 7.9$ Hz, 1H), 7.23 (dt, $J = 5.9, 2.7$ Hz, 3H), 7.15 – 7.05 (m, 3H), 6.89 (dd, $J = 8.1, 2.0$ Hz, 1H), 6.69 (s, 1H), 5.70 (d, $J = 10.4$ Hz, 1H), 2.67

– 1.20 (m, 3H), 1.12 – 0.99 (m, 2H). ¹³C NMR (125 MHz, DMSO-*d*₆) δ 159.13, 157.60, 157.47, 157.22, 157.04, 152.56, 135.19, 130.25, 125.45, 124.35, 124.19, 120.55*2 (*J*_{C-F} = 8.5 Hz), 118.80, 117.69, 116.52*2 (*J*_{C-F} = 23.4 Hz), 113.23, 33.14, 31.78, 25.34, 24.96. HRMS (ESI) *m/z*: [M - H]⁻ Calcd for C₂₄H₂₂FN₂O₃: 405.1620, Found 405.1615.

4.2.37. (3*Z*, 6*Z*)-3-(4-fluorophenoxy) benzylidene-6-(1*H*-imidazol-2-yl) methylene) piperazine-2, 5-dione (**17e**)

15a (100.00 mg, 0.28 mmol), imidazole-2-formaldehyde (32.5 mg, 0.34 mmol), Cs₂CO₃ (137.90 mg, 0.42 mmol), Na₂SO₄ (80.20 mg, 0.56 mmol), DMF (3 ml), 20.8 mg yellow solid with a yield at 19%. MP: 243-245°C. ¹H NMR (500 MHz, DMSO-*d*₆) δ 12.62 (s, 1H), 12.04 (s, 1H), 10.38 (s, 1H), 7.42 (t, *J* = 7.9 Hz, 1H), 7.37 (s, 1H), 7.30 – 7.21 (m, 4H), 7.19 (s, 1H), 7.14 – 7.09 (m, 2H), 6.92 (dd, *J* = 8.1, 2.2 Hz, 1H), 6.79 (s, 1H), 6.54 (s, 1H). ¹³C NMR (125 MHz, DMSO-*d*₆) δ 159.14, 157.23, 157.05, 156.73, 156.60, 152.56, 143.55, 134.98, 130.29, 129.45, 128.07, 126.89, 124.55, 120.54*2 (*J*_{C-F} = 8.5 Hz), 119.04, 118.01, 117.96, 116.54*2 (*J*_{C-F} = 23.4 Hz), 114.42, 98.56. HRMS (ESI) *m/z*: [M + H]⁺ Calcd for C₂₁H₁₆FN₄O₃: 391.1201, Found 391.1204.

4.2.38. (3*Z*, 6*Z*)-3-(4-fluorophenoxy) benzylidene-6-(furan-2-ylmethylene) piperazine-2, 5-dione (**17f**)

15a (100.00 mg, 0.28 mmol), 2-furaldehyde (40.67 mg, 0.42 mmol), Cs₂CO₃ (137.90 mg, 0.42 mmol), Na₂SO₄ (80.20 mg, 0.56 mmol), DMF (3 ml), 51.4 mg yellow solid with a yield at 46%. MP: 212-214°C. ¹H NMR (500 MHz, DMSO-*d*₆) δ 10.38 (s, 1H), 9.55 (s, 1H), 7.91 (s, 1H), 7.41 (t, *J* = 7.9 Hz, 1H), 7.28 (d, *J* = 7.6 Hz, 1H), 7.24 (t, *J* = 8.7 Hz, 2H), 7.19 (s, 1H), 7.12 (dd, *J* = 8.8, 4.4 Hz, 2H), 6.90 (dd, *J* = 11.3, 5.8 Hz, 2H), 6.77 (s, 1H), 6.66 (s, 2H). ¹³C NMR (125 MHz, DMSO-*d*₆) δ 159.15, 157.25, 157.12, 157.05, 156.83, 152.57, 149.89, 144.93, 134.98, 130.30, 126.82, 124.53, 123.72, 120.56*2 (*J*_{C-F} = 8.5 Hz), 118.99, 117.96, 116.55*2 (*J*_{C-F} = 23.3 Hz), 114.47, 114.33, 112.45, 101.89. HRMS (ESI) *m/z*: [M + Na]⁺ Calcd for C₂₂H₁₅FN₂O₄Na: 413.0914, Found 413.0906.

4.2.39. (3*Z*, 6*Z*)-3-(4-fluorophenoxy) benzylidene-6-(thiophen-2-ylmethylene) piperazine-2, 5-dione (**17g**)

15a (100.00 mg, 0.28 mmol), 2-thiophene formaldehyde (47.89 mg, 0.42 mmol), Cs₂CO₃ (137.92 mg, 0.42 mmol), Na₂SO₄ (80.17 mg, 0.56 mmol), DMF (3 ml), 63.2 mg yellow

DMSO-*d*₆) δ 10.40 (s, 1H), 9.91 (s, 1H), 7.73 (d, *J* = 4.9 Hz, 1H), 7.56 (d, *J* = 3.3 Hz, 1H), 7.41 (t, *J* = 7.9 Hz, 1H), 7.29 (d, *J* = 7.6 Hz, 1H), 7.26 – 7.17 (m, 4H), 7.12 (dd, *J* = 8.9, 4.4 Hz, 2H), 6.95 (s, 1H), 6.92 (d, *J* = 8.0 Hz, 1H), 6.76 (s, 1H). ¹³C NMR (125 MHz, DMSO-*d*₆) δ 159.15, 157.86, 157.24, 157.04, 152.56, 135.54, 135.03, 130.27, 129.99, 128.42, 128.32, 127.03, 124.54, 124.46, 120.56 (*J*_{C-F} = 8.5 Hz), 118.96, 117.94, 116.54 (*J*_{C-F} = 23.4 Hz), 114.45, 108.62. HRMS (ESI) *m/z*: [M + H]⁺ Calcd for C₂₂H₁₆FN₂O₃S: 407.0860, Found 407.0866.

4.2.40. (3*Z*, 6*Z*)-3-(4-fluorophenoxy) benzylidene-6-(5-bromofuran-2-yl) methylene) piperazine-2, 5-dione (**17h**)

15a (100.00 mg, 0.28 mmol), 5-bromo-2-furan formaldehyde (74.07 mg, 0.42 mmol), Cs₂CO₃ (137.9 mg, 0.42 mmol), Na₂SO₄ (80.20 mg, 0.56 mmol), DMF (3 ml), 90.9 mg yellow solid with a yield at 68%. MP: 211-214°C. ¹H NMR (500 MHz, DMSO-*d*₆) δ 10.42 (s, 1H), 9.65 (s, 1H), 7.41 (t, *J* = 7.9 Hz, 1H), 7.29 (d, *J* = 7.7 Hz, 1H), 7.26 – 7.21 (m, 2H), 7.20 (s, 1H), 7.14 – 7.08 (m, 2H), 6.95 – 6.90 (m, 2H), 6.79 – 6.75 (m, 2H), 6.58 (s, 1H). ¹³C NMR (125 MHz, DMSO-*d*₆) δ 159.14, 157.23, 157.08, 157.03, 152.54, 151.87, 134.95, 130.27, 126.79, 124.55, 124.23, 123.60, 120.55*2 (*J*_{C-F} = 8.5 Hz), 119.00, 117.98, 116.63, 116.44, 114.54, 101.05. HRMS (ESI) *m/z*: [M - H]⁻ Calcd for C₂₂H₁₃BrFN₂O₄: 467.0048, Found 467.0054.

4.2.41. (3*Z*, 6*Z*)-3-(4-fluorophenoxy) benzylidene-6-(5-chlorofuran-2-yl) methylene) piperazine-2, 5-dione (**17i**)

15a (100.00 mg, 0.28 mmol), 5-methylfurfural (46.61 mg, 0.42 mmol), Cs₂CO₃ (137.9 mg, 0.42 mmol), Na₂SO₄ (80.20 mg, 0.56 mmol), DMF (3 ml), 44.0 mg yellow solid with a yield at 38%. MP: 214-216°C. ¹H NMR (500 MHz, DMSO-*d*₆) δ 10.42 (s, 1H), 9.69 (s, 1H), 7.41 (t, *J* = 7.9 Hz, 1H), 7.29 (d, *J* = 7.7 Hz, 1H), 7.26 – 7.21 (m, 2H), 7.20 (s, 1H), 7.14 – 7.09 (m, 2H), 6.98 (d, *J* = 3.5 Hz, 1H), 6.92 (dd, *J* = 8.1, 2.0 Hz, 1H), 6.77 (s, 1H), 6.68 (d, *J* = 3.6 Hz, 1H), 6.58 (s, 1H). ¹³C NMR (125 MHz, DMSO-*d*₆) δ 159.14, 157.23, 157.07, 157.03, 152.56, 149.71, 136.43, 134.96, 130.28, 126.81, 124.55, 124.23, 120.55 (*J*_{C-F} = 8.5 Hz), 119.00, 117.98, 116.54 (*J*_{C-F} = 23.4 Hz), 116.17, 114.55, 109.72, 101.13. HRMS (ESI) *m/z*: [M - H]⁻ Calcd for C₂₂H₁₃ClFN₂O₄: 423.0553, Found 423.0558.

4.2.42. (3*Z*, 6*Z*)-3-(4-fluorophenoxy) benzylidene-6-(5-nitrofuran-2-yl) methylene) piperazine-2, 5-dione (**17j**)

15a (100.00 mg, 0.28 mmol), 5-nitro-2-furaldehyde (59.70 mg, 0.42 mmol), Cs₂CO₃ (137.90 mg, 0.42 mmol), Na₂SO₄

yield at 7%. MP: 237-240°C. ¹H NMR (500 MHz, DMSO-*d*₆) δ 10.53 (s, 1H), 10.08 (s, 1H), 7.80 (s, 1H), 7.42 (s, 1H), 7.33 – 7.09 (m, 7H), 6.94 (s, 1H), 6.84 (s, 1H), 6.68 (s, 1H). ¹³C NMR (125 MHz, DMSO-*d*₆) δ 159.19, 157.32, 157.05, 156.40, 152.83, 152.57, 151.22, 134.81, 130.34, 129.58, 126.55, 124.77, 120.60*2 (*J*_{C-F} = 8.5 Hz), 119.19, 118.25, 116.61*2 (*J*_{C-F} = 23.4 Hz), 115.95, 115.81, 115.18, 98.86. HRMS (ESI) *m/z*: [M - H]⁻ Calcd for C₂₂H₁₃FN₃O₆: 434.0794, Found 434.0797.

4.2.43. (3*Z*, 6*Z*)-3-(4-fluorophenoxy) benzylidene-6-(5-methylfuran-2-yl) methylene) piperazine-2, 5-dione (**17k**)

15a (100.00 mg, 0.28 mmol), 5-methyl-2-furaldehyde (59.70 mg, 0.42 mmol), Cs₂CO₃ (137.90 mg, 0.42 mmol), Na₂SO₄ (80.20 mg, 0.56 mmol), DMF (3 ml), 37.7 mg yellow solid with a yield at 71%. MP: 184-186°C. ¹H NMR (500 MHz, DMSO-*d*₆) δ 10.32 (s, 1H), 9.60 – 9.35 (m, 1H), 7.41 (t, *J* = 7.9 Hz, 1H), 7.28 (d, *J* = 7.8 Hz, 1H), 7.26 – 7.21 (m, 2H), 7.19 (s, 1H), 7.14 – 7.09 (m, 2H), 6.91 (dd, *J* = 8.1, 2.1 Hz, 1H), 6.78 (d, *J* = 3.3 Hz, 1H), 6.75 (s, 1H), 6.59 (s, 1H), 6.29 (d, *J* = 2.5 Hz, 1H), 2.41 (s, 3H). ¹³C NMR (125 MHz, DMSO-*d*₆) δ 159.14, 157.24, 157.05, 156.74, 154.64, 152.55, 148.53, 135.03, 130.28, 126.91, 124.49, 122.40, 120.55*2 (*J*_{C-F} = 8.5 Hz), 118.95, 117.90, 116.54*2 (*J*_{C-F} = 23.4 Hz), 116.09, 113.98, 108.96, 102.30, 13.71. HRMS (ESI) *m/z*: [M + Na]⁺ Calcd for C₂₃H₁₇FN₂O₄Na: 427.1065, Found 427.1063.

4.2.44. (3*Z*, 6*Z*)-3-(4-fluorobenzoyl) benzylidene-6-(5-methylfuran-2-yl) methylene) piperazine-2, 5-dione (**17l**)

15b (100.00 mg, 0.27 mmol), 5-methyl-2-furaldehyde (45.10 mg, 0.41 mmol), Cs₂CO₃ (133.40 mg, 0.41 mmol), Na₂SO₄ (77.50 mg, 0.55 mmol), DMF (3 ml), 50.6 mg yellow solid with a yield at 44%. MP: 232-234°C. ¹H NMR (500 MHz, DMSO-*d*₆) δ 10.51 (s, 1H), 9.49 (s, 1H), 7.91 (dd, *J* = 8.7, 5.6 Hz, 2H), 7.84 (s, 1H), 7.77 (d, *J* = 7.7 Hz, 1H), 7.65 (d, *J* = 7.7 Hz, 1H), 7.59 (t, *J* = 7.6 Hz, 1H), 7.40 (t, *J* = 8.8 Hz, 2H), 6.84 (s, 1H), 6.78 (d, *J* = 3.3 Hz, 1H), 6.60 (s, 1H), 6.29 (d, *J* = 2.6 Hz, 1H), 2.41 (s, 3H). ¹³C NMR (125 MHz, DMSO-*d*₆) δ 194.14, 165.75, 163.74, 157.38, 156.66, 154.65, 148.54, 137.27, 133.39, 132.77*2 (*J*_{C-F} = 9.4 Hz), 130.19, 128.87, 127.36, 122.42, 116.11, 115.71*2 (*J*_{C-F} = 22.0 Hz), 113.57, 108.97, 102.32, 13.71. HRMS (ESI) *m/z*: [M + H]⁺ Calcd for C₂₄H₁₈FN₂O₄: 417.1245, Found 417.1236.

4.2.45. (3*Z*, 6*Z*)-3-(4-fluorophenoxy) benzylidene-6-(((*tert*-butyldimethylsilyl) oxy) methyl) furan-2-yl) methylene) piperazine-2, 5-dione (**17m**)

butyldimethylsilylmethylolfurfural (101.80 mg, 0.56 mmol), Cs₂CO₃ (137.90 mg, 0.42 mmol), Na₂SO₄ (80.20 mg, 0.56 mmol), DMF (3 ml), 45.1 mg yellow solid with a yield at 30%. MP: 176-178°C. ¹H NMR (500 MHz, DMSO-*d*₆) δ 10.33 (s, 1H), 9.42 (s, 1H), 7.42 (t, *J* = 7.9 Hz, 1H), 7.29 (d, *J* = 7.7 Hz, 1H), 7.26 – 7.21 (m, 2H), 7.19 (s, 1H), 7.14 – 7.09 (m, 2H), 6.92 (dd, *J* = 8.1, 2.1 Hz, 1H), 6.84 (d, *J* = 3.4 Hz, 1H), 6.78 (s, 1H), 6.63 (s, 1H), 6.52 (d, *J* = 3.4 Hz, 1H), 4.75 (s, 2H), 0.88 (s, 9H), 0.10 (s, 6H). ¹³C NMR (125 MHz, DMSO-*d*₆) δ 159.14, 157.67, 157.23, 157.15, 157.04, 156.86, 156.69, 155.95, 152.57, 149.53, 149.26, 135.01, 134.97, 130.28, 126.86, 126.77, 124.52, 123.50, 123.12, 120.58, 120.51, 118.98, 117.93, 116.63, 116.44, 115.48, 115.28, 114.31, 114.14, 110.01, 109.46, 102.06, 101.76, 57.55, 55.71, 25.80, 25.74, 17.96, 17.78, -3.20, -5.27. HRMS (ESI) *m/z*: [M + H]⁺ Calcd for C₂₉H₃₂FN₂O₅Si: 535.2059, Found 535.2054.

4.2.46. (3*Z*, 6*Z*)-3-(4-fluorophenoxy) benzylidene-6-((5-(hydroxymethyl) furan-2-yl) methylene) piperazine-2, 5-dione (**17n**)

The tetrabutylammonium fluoride (TBAF, 1M) (1.35 mL, 0.14 mmol) was added to a solution of ((3*Z*, 6*Z*)-3-(*para*-fluorobenzoyloxy) benzene) methylene-6-(((*tert*-butyldimethylsilyl) hydroxymethylfuran)-2-methylene) piperazine-2, 5-dione (120 mg, 0.22 mmol) in dry THF (3 mL). The mixture was stirred at room temperature in the absence of light. The reaction solution was removed under reduced pressure. The filtration was stirred in methanol at room temperature for 2 h, then moved to 0 °C. The solution was filtered, washed with methanol, and dried in vacuum equipment at 50 °C to obtain 70.2 mg of yellow solid with a yield of 74%. MP: 215-218°C. ¹H NMR (500 MHz, DMSO-*d*₆) δ 10.32 (s, 1H), 9.58 (s, 1H), 7.41 (t, *J* = 7.9 Hz, 1H), 7.29 (d, *J* = 7.7 Hz, 1H), 7.26 – 7.21 (m, 2H), 7.19 (s, 1H), 7.15 – 7.09 (m, 2H), 6.92 (dd, *J* = 8.1, 2.0 Hz, 1H), 6.80 (d, *J* = 3.3 Hz, 1H), 6.78 (s, 1H), 6.64 (s, 1H), 6.47 (d, *J* = 3.3 Hz, 1H), 5.52 (t, *J* = 6.0 Hz, 1H), 4.49 (d, *J* = 6.0 Hz, 2H). ¹³C NMR (125 MHz, DMSO-*d*₆) δ 159.14, 157.67, 157.24, 157.15, 157.05, 156.86, 152.56, 149.27, 135.01, 130.29, 126.87, 124.52, 123.13, 120.56*2 (*J*_{C-F} = 8.5 Hz), 118.98, 117.94, 116.54*2 (*J*_{C-F} = 23.4 Hz), 115.49, 114.15, 109.47, 102.07, 55.72. HRMS (ESI) *m/z*: [M + Na]⁺ Calcd for C₂₃H₁₇FN₂O₅Na: 443.1014, Found 443.1020.

4.2.47. (3*Z*, 6*Z*)-3-(4-fluorophenoxy) benzylidene-6-((5-(methoxymethyl) furan-2-yl) methylene) piperazine-2, 5-dione (**17o**)

(59.30 mg, 0.42 mmol), Cs₂CO₃ (137.90 mg, 0.42 mmol), Na₂SO₄ (80.20 mg, 0.56 mmol), DMF (3.5 ml), 44.5 mg yellow solid with a yield at 36%. MP: 150-152°C. ¹H NMR (500 MHz, DMSO-*d*₆) δ 10.35 (s, 1H), 9.49 (s, 1H), 7.41 (t, *J* = 7.9 Hz, 1H), 7.28 (d, *J* = 7.7 Hz, 1H), 7.26 – 7.21 (m, 2H), 7.19 (s, 1H), 7.14 – 7.08 (m, 2H), 6.91 (dd, *J* = 8.1, 2.1 Hz, 1H), 6.85 (d, *J* = 3.4 Hz, 1H), 6.77 (s, 1H), 6.63 (s, 1H), 6.60 (d, *J* = 3.4 Hz, 1H), 4.48 (s, 2H), 3.29 (s, 3H). ¹³C NMR (125 MHz, DMSO-*d*₆) δ 159.14, 157.24, 157.07, 157.04, 156.83, 153.59, 152.57, 149.93, 134.97, 130.28, 126.81, 124.53, 123.73, 120.55*2 (*J*_{C-F} = 8.5 Hz), 118.99, 117.97, 116.54*2 (*J*_{C-F} = 23.3 Hz), 115.16, 114.33, 111.96, 101.79, 65.43, 57.36. HRMS (ESI) *m/z*: [M + Na]⁺ Calcd for C₂₄H₁₉FN₂O₅Na: 457.1170, Found 457.1171.

4.2.48. (3*Z*, 6*Z*)-3-(4-fluorophenyl) benzylidene-6-((5-methoxymethyl) furan-2-yl)methylene)piperazine-2, 5-dione (**17p**)

15b (100.00 mg, 0.27 mmol), 5-methoxymethylaldehyde (98.40 mg, 0.41 mmol), Cs₂CO₃ (133.40 mg, 0.41 mmol), Na₂SO₄ (77.50 mg, 0.55 mmol), DMF (3.5 ml), 91.0 mg yellow solid with a yield at 75%. MP: 214-216°C. ¹H NMR (500 MHz, DMSO-*d*₆) δ 10.57 (s, 1H), 9.52 (s, 1H), 7.94 – 7.89 (m, 2H), 7.84 (s, 1H), 7.77 (d, *J* = 7.7 Hz, 1H), 7.65 (d, *J* = 7.7 Hz, 1H), 7.59 (t, *J* = 7.7 Hz, 1H), 7.40 (t, *J* = 8.8 Hz, 2H), 6.86 (d, *J* = 4.3 Hz, 2H), 6.64 (s, 1H), 6.61 (d, *J* = 3.4 Hz, 1H), 4.49 (s, 2H), 3.29 (s, 3H). ¹³C NMR (125 MHz, DMSO-*d*₆) δ 194.13, 165.75, 163.75, 157.20, 156.75, 153.60, 149.93, 137.28, 133.42, 133.33, 132.77*2 (*J*_{C-F} = 9.4 Hz), 130.22, 128.87, 127.24, 123.74, 115.71*2 (*J*_{C-F} = 22.0 Hz), 115.18, 113.93, 111.96, 101.81, 65.44, 57.36. HRMS (ESI) *m/z*: [M + H]⁺ Calcd for C₂₅H₂₀FN₂O₅: 447.1351, Found 447.1354.

4.2.49. (3*Z*, 6*Z*)-3-(4-fluorophenoxy) benzylidene-6-(1*H*-benzo[d]imidazol-2-yl)methylene) piperazine-2, 5-dione (**17q**)

15a (100.00 mg, 0.28 mmol), 2-formyl benzimidazole (61.90 mg, 0.42 mmol), Cs₂CO₃ (137.90 mg, 0.42 mmol), Na₂SO₄ (80.20 mg, 0.56 mmol), DMF (3 ml), 42.3 mg yellow solid with a yield at 34%. MP: 245-247°C. ¹H NMR (500 MHz, DMSO-*d*₆) δ 12.89 (s, 1H), 12.25 (s, 1H), 10.58 (s, 1H), 7.77 (dd, *J* = 6.5, 2.0 Hz, 1H), 7.60 – 7.55 (m, 1H), 7.43 (t, *J* = 7.9 Hz, 1H), 7.33 – 7.20 (m, 6H), 7.13 (ddd, *J* = 10.5, 5.3, 3.1 Hz, 2H), 6.94 (dd, *J* = 8.1, 2.1 Hz, 1H), 6.87 (s, 1H), 6.65 (s, 1H). ¹³C NMR (125 MHz, DMSO-*d*₆) δ 159.15, 157.25, 157.05, 156.83, 156.26, 152.55, 149.19, 142.87, 134.85, 132.93, 132.46, 130.30,

118.51, 118.12, 116.55*2 (*J*_{C-F} = 23.3 Hz), 115.36, 111.64, 97.33. HRMS (ESI) *m/z*: [M + H]⁺ Calcd for C₂₅H₁₈FN₄O₃: 441.1357, Found 441.1350.

4.2.50. (3*Z*, 6*Z*)-3-(4-fluorophenoxy) benzylidene-6-(benzofuran-2-yl methylene) piperazine-2, 5-dione (**17r**)

15a (100.00 mg, 0.28 mmol), benzofuran-2-formaldehyde (61.90 mg, 0.42 mmol), Cs₂CO₃ (137.90 mg, 0.42 mmol), Na₂SO₄ (80.20 mg, 0.56 mmol), DMF (3 ml), 76.5 mg yellow solid with a yield at 61%. MP: 254-256°C. ¹H NMR (500 MHz, DMSO-*d*₆) δ 10.51 (s, 1H), 9.91 (s, 1H), 7.74 (d, *J* = 8.5 Hz, 1H), 7.68 (d, *J* = 7.7 Hz, 1H), 7.43 (t, *J* = 7.9 Hz, 1H), 7.40 – 7.36 (m, 1H), 7.33 – 7.28 (m, 3H), 7.24 (d, *J* = 8.7 Hz, 3H), 7.15 – 7.11 (m, 2H), 6.93 (dd, *J* = 8.0, 2.1 Hz, 1H), 6.82 (s, 1H), 6.80 (s, 1H). ¹³C NMR (125 MHz, DMSO-*d*₆) δ 159.15, 157.25, 157.05, 156.92, 156.86, 154.64, 152.56, 151.88, 134.94, 130.28, 127.76, 126.77, 126.36, 125.72, 124.58, 123.64, 121.43, 120.57*2 (*J*_{C-F} = 8.5 Hz), 119.03, 118.02, 116.54*2 (*J*_{C-F} = 23.3 Hz), 114.79, 111.59, 110.05, 101.43. HRMS (ESI) *m/z*: [M + H]⁺ Calcd for C₂₆H₁₈FN₂O₄: 441.1245, Found 441.1243.

4.3. Biology

4.3.1. Anticancer activities

Human cancer cell lines were purchased from American Type Cell Culture Collection (ATCC, USA). Cells were maintained in DMEM medium supplemented with 10% (v/v) heat-inactivated fetal bovine serum, penicillin-streptomycin (100 U/mL-100 g/mL) and 2 mM glutamine at 37°C in a humidified atmosphere (5% CO₂-95% air). Cells (5 × 10³ per well) were seeded in 96-well plates for 24 h. All test derivatives were dissolved in 100% cell culture grade DMSO. After incubation cells were treated with test compounds for 72 h. Cell viability was assessed by MTT assay. The absorbance at 490 nm was measured with a Microplate Reader (Molecular Devices, Silicon Valley, USA). The data was analyzed by Origin 8.5.

4.3.2. Immunofluorescence assay

NCI-H460 cells were seeded in a 24-well plate (with coverslips plated) at a density of 5 × 10⁴ cells. After overnight adherence, the cells were exposed to compounds at 5 nM or 10 nM for 24 h. Then, the cells were fixed with 4% cold paraformaldehyde at 4 °C for 15 min and then permeabilized in 0.05 % Triton X-100 for 10 min. The cells were blocked in 1 % BSA for 30 min. Microtubules were detected by incubation with

washed with PBS and incubated with a FITC-conjugated anti-mouse IgG antibody. Nuclei were stained with DAPI (G1012, Servicebio, China). The coverslips were visualized under a fluorescence microscope (Nikon Eclipse C1, Nikon, Japan) and image-forming system (Nikon DS-U3, Nikon, Japan).

4.4. Molecular modeling

Ligands were prepared using the QuickPrep module in Maestro and energy was minimized through the general method. Theoretical calculations of the physical properties (QpLogPo/w and QpPCaco) of these synthesized compounds were performed using the Qikprop Module of Maestro software. The X-ray crystallographic structure was retrieved from the protein data bank (PDB: 5XHC) at a resolution of 2.75 Å. The protein domain subunits C and D and all water molecules were removed using Maestro 11.5 using the protein preparation refinement module. A subsequent energy minimization was carried out using the OPLS_2005 force field. Then, molecules were docked into the co-crystal structure of tubulin-compound 1.

The docking position was constrained by hydrogen bond using the receptor grid generation module. Molecular modeling was made by the ligand docking module according to imports from the pretreatment ligand and the protein. At least 5 poses for each compound were retained, and the best poses of rigid docking and induced fit docking were refined.

Acknowledgments

This work was supported by “Zhufeng Scholar Program” of Ocean University of China (841412016), and Aoshan Talents Cultivation Program of Qingdao National Laboratory for Marine Science and Technology (No. 2017ASTCP-OS08) to Dr. Wenbao Li. We also acknowledge that the supports provided by Ms Xiaoxiao Xu, Zhenhua Tian and Mr. Sifeng Zhu.

References

1. AACR cancer progress report 2019. **2019**. https://cancerprogressreport.org/Documents/AACR_CPR_2019.pdf
2. Zhou J, Giannakakou P. *Current Medicinal Chemistry-Anti-Cancer Agents*, **2005**, 5(1):65-71.
3. Dumontet C, Jordan M A. *Nature Reviews Drug Discovery*, **2010**, 9(10):790-803.
4. Guo H, Li X, Guo Y, et al. *Medicinal Chemistry Research*, **2019**, 28(7):927-937.
5. Downing K H. *Current Opinion in Structural Biology*, **1998**, 8(6):785-91.
6. Nogales E. *Annual Review of Biochemistry*, **2000**, 69(1):277-302.
7. 339(6119):587-590.
8. Daniele F, Giuseppe B, Francesco P, et al. *Analytical Cellular Pathology*, **2015**, 1-19.
9. Raffaele D F, Luigi A, Salvo D M, et al. *Frontiers in Pharmacology*, **2017**, 8:797.
10. Kanoh K, Kohno S, Katada J, Hayashi Y, Muramatsu M, Uno I. *Bioscience Biotechnology and Biochemistry*, **1999**, 63(6):1130-1133.
11. Kanoh K, Kohno S, Katada J, et al. *Bioorganic & Medicinal Chemistry*, **1999**, 7(7):1451-1457.
12. Singh A V, Bandi M, Raje N, et al. *Blood*, **2011**, 117(21):5692-5700.
13. Yamazaki Y, Tanaka K, Nicholson B, et al. *Journal of Medicinal Chemistry*, **2012**, 55(3):1056-71.
14. Nicholson B, Lloyd G K, Miller B R, et al. *Anti-Cancer Drugs*, **2006**, 17(1):25-31.
15. Giuseppina L S, Natacha O, Ashwani S, et al. *Nature Chemistry*, **2019**, 5(11):2969-2986.
16. Kashyap A S, Fernandez-Rodriguez L, Zhao Y, et al. *Cell Reports*, **2019**, 28(13):3367-3380.e8
17. Wang Y X, Zhang H, Gigant B, et al. *FEBS Journal*, **2016**, 283(1):102-111.
18. Fu Z Y, Hou Y W, Ji C P, et al. *Bioorganic & Medicinal Chemistry*, **2018**, 26(8):2061-2072.
19. Tian Z H, Chu Y Y, Wang H, et al. *RSC Advances*, **2018**, 8(2):1055-1064.
20. Ding Z P, Ma M X, Zhong C J, et al. *Bioorganic & Medicinal Chemistry*, **2019**. DOI: 10.1016/j.bmc.2019.115186.
21. Ma M X, Ding Z P, Wang S X, et al. *Bioorganic & Medicinal Chemistry*, **2019**, 17:1836-1844.
22. Yamazaki Y, Sumikura M, Masuda Y, et al. *Bioorganic & Medicinal Chemistry*, **2012**, 20(14):4279-4289.
23. Hayashi Y, Takeno H, Chinen T, et al. *ACS Medicinal Chemistry Letters*, **2014**, 5(10):1094-1098.
24. Xu G Y G., Pagare P P., Ghatge M S., et al. *Molecular Pharmaceutics*, **2017**, 14(10):3499-3511.

Dear Editors:

This is a manuscript entitled “**Structure-based design and synthesis of novel furan-diketopiperazine-type derivatives as potent microtubule inhibitors for treating cancer**”.

There is no conflict of interest exists in submission of this manuscript. I would like to declare on behalf of my co-authors that the work described is original research that has not been published in whole or in part previously. And, this manuscript is approved by all authors for publication.